Schwinger pair production and fall to the center

By

Sriram Sundaram

Department of Physics
McMaster University

A dissertation submitted to McMaster University in accordance with the requirements of the degree of Master of Science in the Faculty of Science.

August 2019

McMaster University
Department of
Physics & Astronomy

Information and Declaration

McMaster University Master of Science (2019)
Hamilton, Ontario, Canada
Department of Physics

Title: Schwinger pair production and fall to the center
Author: Sriram Sundaram.
Supervisor: Professor Duncan H. J. O'Dell
Number of Pages: xiv, 48

I, the author, hereby certify that the work in this dissertation is, unless otherwise acknowledged through citation, original and has not been otherwise submitted for any academic degree or qualification. Any ideas, techniques, or other materials belonging to others are explicitly referenced in the text. Any views expressed in the dissertation are those of the author.

Abstract

The classical field theory of Schwinger pair creation can be described using an effective Schrödinger equation with an inverted harmonic oscillator Hamiltonian [1, 2]. It is a well known fact that the inverted harmonic oscillator admits a canonical transformation to a $Q.P$ type Berry-Keating Hamiltonian [3]. In this thesis we demonstrate that the classical field theory of Schwinger pair creation has a hidden scale invariance described by the quantum mechanics of an attractive inverse square potential in the canonically rotated (Q, P) coordinates of the inverted harmonic oscillator. The quantum mechanics of the inverse square potential is well known because of the problem of fall to the center and the associated ambiguities in the boundary condition. It is also well known as a description of the physics of pair creation in the presence of an event horizon [2] and black hole decay. We use point particle effective field theory (PPEFT) to derive the boundary condition which describes pair creation. This leads to the addition of an inevitable Dirac delta function with imaginary coupling to the inverse square potential, describing the physics of the source. This non-hermitian physics leads to the Klein paradox. The conservation loss is due to the charged pairs being produced during tunneling.

Acknowledgements

I would like to thank my supervisor Prof. Duncan O'Dell for being a guide and a teacher to the true sense of the word. Thanks to him for giving me the freedom to explore this subject broadly and in depth. His support, trust and patience was instrumental in shaping this project to what it is now. I would also like to thank Prof. Cliff Burgess and Prof. Erik Sorenson for being a part of my research supervisory committee and for the motivating comments to pursue this project. I would like to express my gratitude to Professor Emeritus Rajat Bhaduri (and his family) and Professor Emeritus Donald Sprung for many fruitful conversations. When I see them working I realize physicists never retire. I would also like to acknowledge Dr. Mainak Sadhukhan (Indian Institute of Technology Kanpur, India) and Dr. Vivek Vyas (Raman Research Institute, Bengaluru, India) for many fruitful discussions. Such all the time support and affection are priceless. I would also like to thank Prof. Prasanta K. Panigrahi (Indian Institute of Science Education and Research Kolkata, India) for being a good mentor and a teacher and for suggesting related references for this project. Thanks to Dr. Ritesh K. Singh (Indian Institute of Science Education and Research Kolkata, India) for being a motivating teacher. Thanks to Peter Hayman, Ryan Plestid, Wyatt Kirkby and Matt Richards for many helpful conversations.

All of this wouldn't have been possible without the strong support of my parents Sundaram Raman and Chithra Narayanan. Love to my sister Rajalakshmi Sundaram and my brother-in-law Hareesh Parthasarathy for being there for me always. I would also like to thank my brother Varun, my Uncle Rajesh Raman, Aunty Sudha Rajesh and my parents for not letting me miss them. Thanks to my Uncle Balan Narayanan who is my role model for many aspects in life. Thanks to my good friends Abhijit Chatterjee, Ananya Krishnan and Lekshmi for their support. Thanks to my landord Dr. Binoy Prasad and Reeta Prasad for providing me a peaceful place to live in Hamilton. Last but not the least my Grandparents (S Raman (Late) and G Rajalakshmi, H S Narayanan (Late) and Sathyabhama), have always been a source of inspiration for me.

Dedication

To my grandparents, parents and my family who are my source of inspiration and strength. To all my teachers who taught me the importance of knowing.

Table of Contents

List of Tables

List of Figures

CHAPTER 1

Introduction

The instability of the vacuum of quantum field theory in the presence of a static electric field that creates charged pairs is termed as Schwinger pair production. Dirac proposed that the negative energy solutions be identified with antiparticle (positron) in 1931. After Dirac's work on relativistic theory of electron, Euler and Heisenberg initiated the study of quantum fluctuations in the Dirac sea picture of the vacuum of quantum field theory [4, 5]. Feynman-Stückelberg further proposed a physical picture in which antiparticles propagate backward in time :

" *the negative energy states appear in a form which may be pictured (as by Stückelberg) in space-time as waves travelling away from the external potential backward in time* " [6].

Related to this is Yoichiro Nambu's famous remark on pair creation [8] :

" *the eventual creation and annihilation of pairs that may occur now and then is no creation or annihilation, but only a change of direction of moving particles, from the past to the future, or from the future to the past*"

In 1951, Julian Schwinger, reformulated Heisenberg and Euler's work in a paper "On gauge invariance and vacuum polarization"which deals with study of Green's functions, renormalization and gauge invariance [7]. Schwinger pair production has a long history of close to 80 years [8]. In the classical field theory of Schwinger pair production, over-reflection of charged particles (the well known Klein paradox [9]) from a barrier formed from an inhomogeneous electric field is reconciled by pair creation. Probability conservation is then reinterpreted as charge conservation. Even though there has recently been a proposal for experimentally realizing analog to pair creation [10], it has not yet been realized.

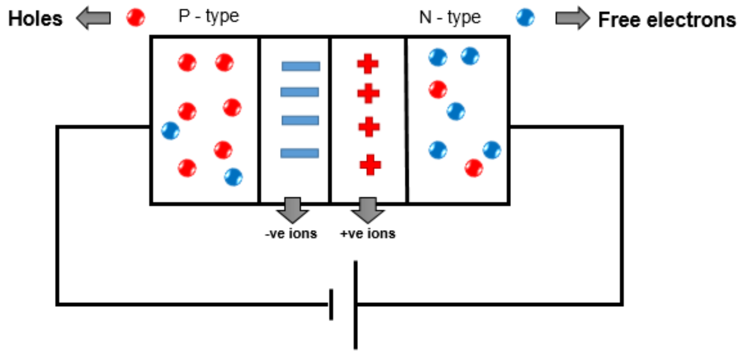

Figure 1.1: Zener breakdown - The picture depicts a reverse biased, heavily doped pn-junction diode whose width of the depletion region increases with the increase in the reverse bias voltage. The resulting electric field when strong enough knocks out charged particles from the crystals and it tunnels through the depletion region which results in a huge rush of current through the circuit and the diode breaks down.

The classical field theory of Schwinger pair creation can be described using an effective Schrödinger equation with an inverted harmonic oscillator (IHO) [1] potential which illustrates an unstable equilibrium. The quantum mechanics of the IHO as a simple description of unstable equilibrium has been studied extensively since Barton [11]. The IHO gives a fall to infinity where a particle rolls down to infinity from the top of the parabolic barrier. The particle production happens during the tunneling of charged particles when the external field is strong enough [1]. The Zener breakdown of a heavily doped reverse biased pn-junction diode is an example where tunneling of charged particles occurs through the junction in the presence of a static electric field [see Figure 1.1]. The energy eigenfunctions of the IHO are the parabolic cylinder functions [11] whose properties and asymptotics are well known. It is considered as a well-posed self-adjoint problem but it is physically pathological because it has infinitely negative energy states. Self-adjointness is usually not distinguished from hermiticity of an operator. Self-adjointness requires the domain of the operator and its adjoint to be the same, i.e $D(A) = D(A^\dagger)$. The mathematical recipe used to test whether an hermitian operator is self-adjoint is von Neumann's test using deficiency indices [12] (for details see Appendix A). For non-self adjoint operators, usually the suggested remedy is to implement a self-adjoint extension, which is however, not unique [13, 14].

Canonical transformations are well known tools used in classical and quantum physics [15] to bring out the hidden symmetries of the system [16]. The form of the equations of motion are invariant under a canonical transformation, so the dynamics is equivalent. The quantum version started gaining attention with the introduction of the quantum Hamilton-Jacobi formalism [17–19] (for details, see Appendix C). It is a well known fact that the inverted harmonic oscillator admits a canonical transformation to $H(Q, P) = Q.P$ type Hamiltonian [3]. The classical phase space portrait of the inverted harmonic oscillator, or equivalently

$H(Q,P) = Q.P$, is hyperbolic in nature. The quantum mechanics of $H(Q,P) = Q.P$ type Hamiltonian gained huge attention after the paper by Berry and Keating [20], proposing it as a candidate which generates Riemann zeros, but it is still a debated issue. For this reason, $H = Q.P$ is sometimes termed as the Berry-Keating operator in the literature. In this thesis we refer to $H = Q.P$ as the Berry-Keating Hamiltonian. Pair production is usually described as tunneling process between the Rindler like disconnected space time sectors [2]. Interestingly, apart from the mapping to a $Q.P$ type Hamiltonian, recently the inverted harmonic oscillator has been mapped under a time dependent canonical transformation to a particle in a box with moving walls [21].

Bertrand's theorem states that among central force potentials with bound orbits, the only two central potentials that admit closed orbits are simple harmonic oscillator and the Kepler potential. Unlike these, the inverse square potential is well known for the physics of fall to the center where the particle spirals onto the origin [22]. The relationship between the simple harmonic oscillator and Kepler potential have been the subject of investigation since Newton, Hooke and Bertrand (for references see : [23]). It is a known fact that the Kepler problem can be mapped to a simple harmonic oscillator and is still a subject of extensive study in quantum physics [24]. However, the mapping between the inverted harmonic oscillator Hamiltonian and the inverse square Hamiltonian is not been studied as far as we know.

The quantum mechanics of the inverse square potential has been a subject of investigation since reference [25]. It appears in the physics of gravitating systems, black holes [26], charged wire [27] etc. It is known to have a hidden SU(1,1) spectrum generating symmetry, which is often termed as Pitaevskii-Rosch symmetry [28]. The Schrödinger equation with an inverse square potential exhibits scale invariance in contrast to other well known potentials like the simple harmonic oscillator, the inverted harmonic oscillator, the coulomb potential etc. The quantum mechanics of inverse square potentials is well known for the ambiguity in choosing the right boundary condition and renormalization effects [29]. It appears that the inverse square potential by itself is not a fully specified eigenvalue problem as one needs to specify a boundary condition at the origin to make the quantum problem well posed. Infact, one is inevitably led to add a Dirac delta function at the origin to make the inverse-square problem fully specified [30].

In this thesis we demonstrate that the classical field theory of Schwinger pair creation has a hidden scale invariance. In the first chapter we obtain the quantum inverted harmonic oscillator in an effective Schrödinger equation. A canonical transformation to a scale invariant Schrödinger equation with an attractive inverse square potential using a squared Berry-Keating operator is then shown. One needs to specify a boundary condition at the origin to make the quantum problem of an inverse square potential well posed. In the following chapter, point particle effective field theory (PPEFT) is used to systematically derive the boundary condition. We then illustrate the non-hermitian physics (which leads to the Klein paradox) using the inevitable Dirac delta function with imaginary coupling describing the physics at the source ($Q = 0$), of the attractive inverse square potential.

At the end, we also explore the su(1,1) Lie algebra generated by the inverted harmonic oscillator, simple harmonic oscillator and Berry-Keating operator, which gives the hint that pair creation can be considered as squeezing of the vacuum. In the branch of quantum optics, the parabolic cylinder functions are known to be squeezed states constructed out of mixed excitation and deexcitation operators of SU(1,1) group as discussed in [31]. We explicitly show that the energy eigenvalue problem of the inverted harmonic oscillator Hamiltonian can itself be naturally identified as the eigenvalue problem for determining squeezed states.

CHAPTER 2

Inverted harmonic oscillator and hidden scale invariance

2.1 Inverted harmonic oscillator and the Berry-Keating Hamiltonian

Consider a classical scalar field $\phi(x,t)$ of charge q, which satisfies Klein-Gordon equation in 1+1 dimension in the presence of a static electric field of strength E, with the gauge choice $A_0 = -Ex$, $A_x = 0$ [1,32] :

$$\left(\hbar^2 \frac{\partial^2}{\partial x^2} - \left(\frac{\hbar}{c}\frac{\partial}{\partial t} + \frac{\mathrm{i}qEx}{c}\right)^2\right)\phi(x,t) = m^2c^2\phi(x,t) \tag{2.1}$$

For a given mode $\phi_\omega(x,t) = \exp(-\mathrm{i}\omega t)f_\omega(x)$, $f_\omega(x) = \langle x|\phi\rangle$, satisfies a Schrödinger equation with an inverted harmonic oscillator (IHO) potential :

$$\left(\frac{-\hbar^2}{2m}\frac{\partial^2}{\partial x^2} - \frac{1}{2}m\left(\frac{qE}{mc}\right)^2\left(x - \frac{\hbar\omega}{qE}\right)^2\right)\langle x|\phi\rangle = \frac{-mc^2}{2}\langle x|\phi\rangle \tag{2.2}$$

Redefining the variable, $\xi = \sqrt{\frac{|q|E}{\hbar c}}\left(x - \frac{\hbar\omega}{qE}\right)$,

$$\hat{H}(\pi,\xi)\langle\xi|\phi\rangle = \frac{\pi^2 - \xi^2}{2}\langle\xi|\phi\rangle = -\tilde{E}\langle\xi|\phi\rangle \tag{2.3}$$

where[1], $\pi = -\mathrm{i}\frac{\partial}{\partial\xi}$ with $[\pi,\xi] = -\mathrm{i}$ and $\tilde{E} = \frac{m^2c^3}{|q|E\hbar}$. The IHO gives a fall to infinity. By contrast, in this thesis we intend to show the mapping of this model of instability to a fall to

[1] Beware : changing $E \to -E$ (equivalently : $q \to -q$) does not change $\tilde{E} \to -\tilde{E}$ as seems to be implied by Eq. (2.3), so the quantum problem is still a "tunneling problem". Also Eq. (2.2) is invariant under $q \to -q$ and $x \to -x$, i.e. CP symmetry.

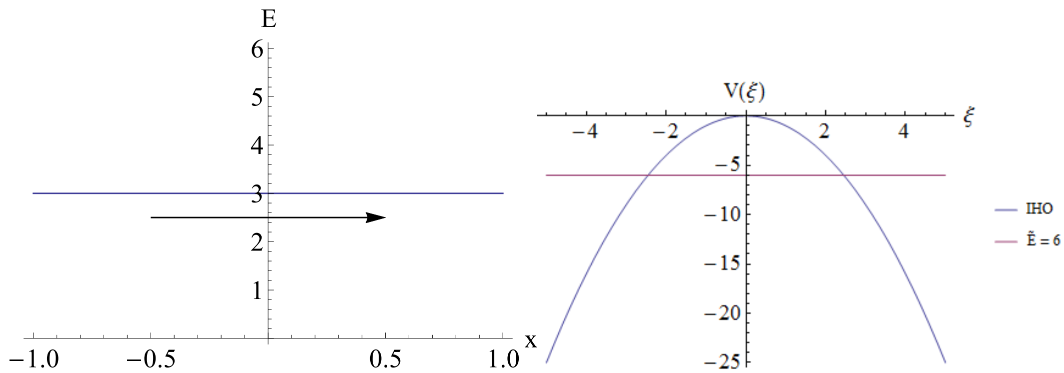

(a) (b)

Figure 2.1: (a). Constant electric field of strength $E = 3$, with the arrow indicating the direction of the electric field. (b). Inverted harmonic oscillator potential, with $V(\xi) = -\xi^2$, $\tilde{E} = 6$ which falls off to infinity.

the center. The energy eigenstates of the IHO Hamiltonian are well known to be parabolic cylinder functions ($\phi(\xi) = \alpha W(\tilde{E}, \xi) + \beta W(\tilde{E}, -\xi)$, α, β are constants). [11]. However, to describe the physics of pair creation one needs to include both positive and negative energy states. Using the standard scattering description of the IHO, its not trivial, at least at first sight, as to which parabolic cylinder function corresponds to the particle and anti-particle states. It seems that one needs more information (boundary conditions) to describe the physics of pair creation. In this thesis we set up the boundary condition in the canonically rotated coordinates. The IHO Hamiltonian admits a canonical transformation [3] :

$$Q = \frac{\pi + \xi}{\sqrt{2}}, P = \frac{\pi - \xi}{\sqrt{2}}, \tag{2.4}$$

which preserves the classical Poisson bracket, $\{Q, P\} = 1$, and hence $[\hat{Q}, \hat{P}] = \mathrm{i}$. Note that, unlike in the related case of the simple harmonic oscillator, the operators Q and P are Hermitian. The Hamiltonian with an IHO potential can now be written in terms of the new coordinates as :

$$\hat{H}(\hat{Q}, \hat{P}) = \frac{\hat{Q}.\hat{P} + \hat{P}.\hat{Q}}{2} \tag{2.5}$$

This Berry-Keating type Hamiltonian admits classical orbits given by, $P = \sqrt{\tilde{E}}\exp(-t)$ and $Q = -\sqrt{\tilde{E}}\exp(t)$. The classical phase space for $H(Q, P) = Q.P$ has disconnected sectors similar to dynamics in Rindler coordinates [see Figure 2.2 (a)]. In the Q-representation, with $\hat{Q}\,|Q\rangle = Q\,|Q\rangle$ and $\hat{P} = -\mathrm{i}\frac{\partial}{\partial Q}$, the Schrödinger equation for the IHO [Eq. (2.3)] takes the form :

$$Q\frac{\partial}{\partial Q}\langle Q|\phi\rangle = \left(-\mathrm{i}\tilde{E} - \frac{1}{2}\right)\langle Q|\phi\rangle \tag{2.6}$$

which is scale invariant, i.e. is invariant under $Q \to \lambda Q$, unlike the Schrödinger equation with IHO potential.

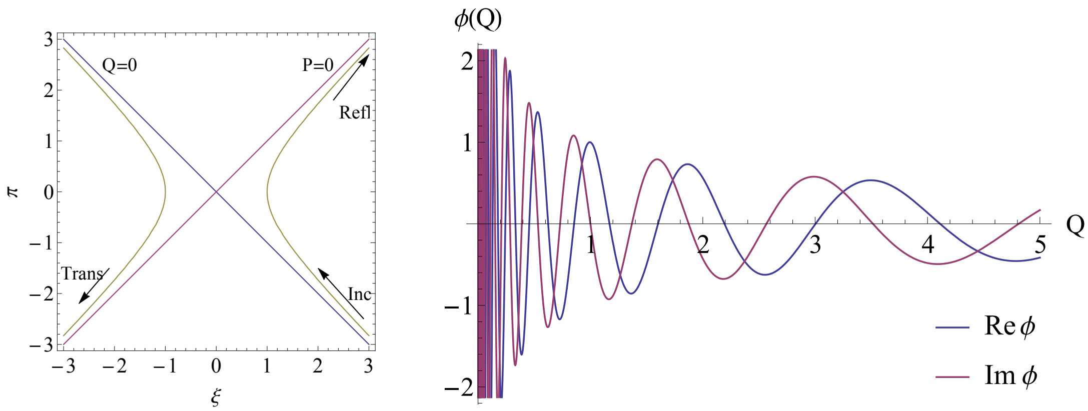

(a) (b)

Figure 2.2: (a). Classical phase space of IHO. The classical hyperbolic orbits are given by $P = P_0 \exp(-t)$ and $Q = Q_0 \exp(t)$, with $Q_0 P_0 = -\tilde{E}$. At early times $t \to -\infty$, with $P = -\sqrt{\tilde{E}} e^{-t}$ and $Q = \sqrt{\tilde{E}} e^{t}$, orbits near $P \to -\infty$ and $Q \to 0^+$,incoming wave (from $\xi = +\infty$) is then described by $C = 0$ in Eq. (2.9) (Inc branch in the figure) and as $t \to \infty$, $Q \to \infty$ and $P \to 0$ (reflected, Refl branch in the figure). However, in quantum mechanics we also have transmitted wave corresponding to $P \to 0$ and $Q \to -\infty$ (transmitted, Trans branch with $Q = -\sqrt{\tilde{E}} e^{t}$ and $P = \sqrt{\tilde{E}} e^{-t}$ in the figure). (b). Wavefunction of the $H(Q, P)$ in the Q-representation which exhibit both amplitude and logarithmic phase singularity at Q = 0. The phase singularity is due to the term $\exp(\mathrm{i}\tilde{E}\ln(Q))$ that appears in the Eq. (2.7) .

The wavefunction in the Q-representation is :

$$\langle Q|\phi\rangle = A\,\Theta(Q)\,Q^{-\mathrm{i}\tilde{E}-\frac{1}{2}} + B\,\Theta(-Q)\,(-Q)^{-\mathrm{i}\tilde{E}-\frac{1}{2}} \tag{2.7}$$

where $\Theta(Q)$ is the Heaviside step function. The step function $\Theta(Q)$ is required in writing the wavefunction because the Berry-Keating Hamiltonian is essentially self-adjoint in the half real line ($\mathbb{R}^{\pm}$) and not on the full real line ($\mathbb{R}$) [see Appendix A for the details] [33]. Waves of the form $Q^{i\nu} = \exp(i\nu \ln[Q])$ with $Re(\nu) \neq 0$ exhibit a logarithmic phase singularity and are signatures of quantum catastrophes [34]. The above wavefunction exhibits a logarithmic phase singularity [see Figure 2.2 (b)]. Such singularities also appear in waves near the event horizon of a black hole, in accelerated frames, etc. Similarly, the Schrödinger equation in the P-representation is given by :

$$P\frac{\partial}{\partial P}\langle P|\phi\rangle = \left(\mathrm{i}\tilde{E} - \frac{1}{2}\right)\langle P|\phi\rangle \tag{2.8}$$

The Berry-Keating Hamiltonian is symmetric under the exchange of Q and P, like the simple harmonic oscillator Hamiltonian. The Schrödinger equation in the Q-representation then only differs from the P-representation in i $\to$ −i, i.e. time reversal. Hence, one representation describes the particle states and the other the anti-particle states in accordance with the Feynman-Stückelberg interpretation. One can construct the wavefunction in the

P-representation from Eq. (2.8) as :

$$\langle P|\phi\rangle = C\,\Theta(P)\,P^{\mathrm{i}\tilde{E}-\frac{1}{2}} + D\,\Theta(-P)\,(-P)^{\mathrm{i}\tilde{E}-\frac{1}{2}} \tag{2.9}$$

We have to choose either $C = 0$ or $D = 0$ to identify this wavefunction as an incident wave [see the classical phase space portrait Figure 2.2 (a) which shows the incident, reflected and transmitted branches]. Computing the Fourier transform of the wavefunction in the P-representation by doing a continuation across the singularity at $Q = 0$, we can get the wavefunction in the Q-representation Eq. (2.7) with the ratio of reflection and transmission coefficient satisfying, $\left|\frac{A}{B}\right| = e^{\tilde{E}\pi}$ [1].

One can choose to work with the above two first-order differential equations to describe the problem, which is usually preferred as discussed in [1,32]. However, here we describe the Schwinger pair creation problem using a single second order differential equation by mapping it to a Schrödinger equation with an inverse square potential and we implement the boundary condition using point particle effective field theory. Squaring allows one to combine both the positive and negative energy solutions in a single second order differential equation.

2.2 Squared Berry-Keating operator and Hamiltonian with an inverse square potential

Consider the second order differential equation :

$$\left(\frac{\hat{Q}.\hat{P} + \hat{P}.\hat{Q}}{2}\right)^2 |\phi\rangle = \tilde{E}^2\,|\phi\rangle \tag{2.10}$$

Taking the square root of the above Hamiltonian, naturally gives the Berry-Keating Hamiltonian, $H(Q,P) = \frac{Q.P+P.Q}{2}$, with positive or negative energy eigenvalue. The Berry-Keating Hamiltonian $H(Q,P) = \frac{Q.P+P.Q}{2}$ is not time reversal invariant because $P \to -P$ under time reversal. Hence, this squared Berry-Keating Hamiltonian has the information of both particles and antiparticles. In the Q-representation the Schrödinger equation Eq. (2.10), can be written as :

$$\left(Q^2\frac{d^2}{dQ^2} + 2\,Q\frac{d}{dQ} + (\tilde{E}^2 + 1/4)\right)\phi(Q) = 0 \tag{2.11}$$

This differential equation is scale invariant which gives us a hint about a hidden inverse square potential present. Transforming the above differential equation by putting $\phi(Q) = Q^{-1}\chi(Q)$, we get

$$-\frac{d^2\chi(Q)}{dQ^2} - \frac{(\tilde{E}^2 + 1/4)}{Q^2}\chi(Q) = 0 \tag{2.12}$$

we add $\mathcal{E}\chi(Q)$ to make a strict analogy to the Schrödinger equation with an attractive inverse square potential,

$$-\frac{d^2\chi(Q)}{dQ^2} - \frac{(\tilde{E}^2 + 1/4)}{Q^2}\chi(Q) = \mathcal{E}\chi(Q) \tag{2.13}$$

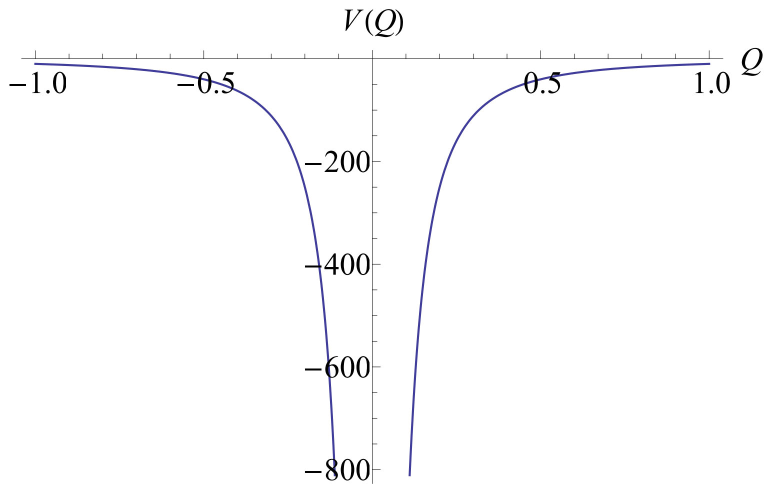

Figure 2.3: Plot of attractive inverse square potential in the canonically rotated Q coordinate : $V(Q) \propto -\frac{1}{Q^2}$

The small Q limit of the above Schrödinger equation [Eq. (2.13)] will amount to neglecting the energy eigenvalue $\mathcal{E}$, compared to the potential energy, leading to Eq. (2.12) with zero energy eigenvalue. Here, we have demonstrated that the classical field theory of Schwinger pair production has a hidden quantum mechanics of an attractive inverse square potential. The above Schrödinger equation is well known for its scale invariance, i.e. under the scale transformation $Q \to \lambda Q$, and the ambiguity in choosing the boundary condition. The wavefunction for small Q exhibits a logarithmic phase singularity, like Eq. (2.7) for $H(Q, P) = \frac{Q.P+P.Q}{2}$, which we will make explicit in the next section. This is a quantum manifestation of fall to the center, where one needs to specify a boundary condition at the origin $Q = 0$, to choose the coefficients of the linearly independent wavefunctions. The ambiguity in determining the boundary condition arises from the fact that the Hamiltonian fails to be self-adjoint (see Appendix A). The usual prescription to surmount this problem is to impose self adjoint extensions. However, self-adjoint extensions are not unique and furthermore would not describe particle production. This is where point particle effective action which describes the physics of the source comes to the rescue, as illustrated by Burgess et. al [30]. In the next chapter of the thesis, we show that Schwinger pair creation due to an electric field can also be described using the above attractive inverse square potential in the framework of point particle effective field theory, developed by Burgess et. al [30].

Chapter 3

Point particle effective field theory and inverse square potential

Effective field theory describes physical phenomenon occurring at a chosen length scale or energy scale including the appropriate degrees of freedom while ignoring the substructures and degrees of freedom at shorter distances (or high energies). Effective field theory has found applications in various disciplines such as the standard model of particle physics and also in non-relativistic quantum mechanics. Effective field theory works well when there is a relatively large separation between the length scale of interest and the length scale of the microscopic physics. For example, to describe the motion of electrons around the nucleus of an atom (of radius a, say), it is natural to neglect the internal structure of the nucleus (of radius r, see Figure 3.1) and instead focus on their motion about a point-like nucleus whose internal structure is described by a multipole expansion. When $r/a << 1$, one can largely be ignorant about the structure of the nucleus (source).

The effective action will have the form $S = S_B + S_b$, where S_B describes the action of the bulk field while S_b is the point particle action of the source. Effects of particle substructures can be incorporated by additional interactions in S_b which is a generalized multipole expansion for the source. Such expansions have been studied in the context of gravity (see references in [30]). Burgess et al. in [30], using PPEFT for an attractive inverse square potential, provide a systematic algorithm that relates the properties of the effective action at the origin, $Q = 0$ to the boundary condition at $Q = 0$. Before implementing PPEFT to the problem of Schwinger pair creation, we explain briefly the conceptual benefits of applying PPEFT to the inverse square problem. Since it is cast in terms of an effective action, it removes the guesswork that is otherwise required in implementing the boundary conditions. Casting it in terms of an action provides a physical basis for determining the right choice of source action that is required. An added advantage of using a PPEFT is the transparency as

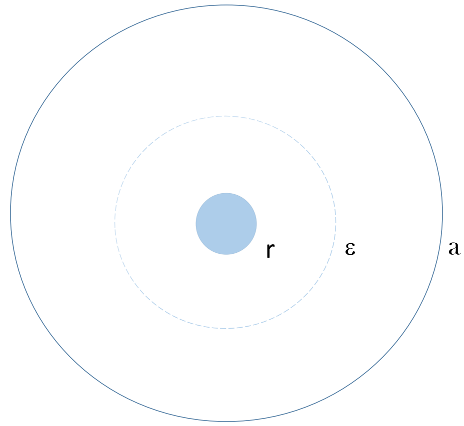

Figure 3.1: Picture depicting hierarchy of scales present when deriving boundary condition from the source action. Here, r denotes the size of the source (eg : size of a proton/nucleus) and a denotes the physical length scale of the problem (eg: size of the atom). Size of the source is assumed to be very small compared to physical scale, a. PPEFT uses action of point source to derive boundary condition at the hypothetical surface of radius ϵ, which is arbitrary. Renormalization group flow describes how the effective coupling within PPEFT action must change for different values of ϵ in order to keep physical quantities remain unchanged.

to which quantity is renormalized. From the point particle effective action, it is the effective contact coupling that is renormalized, which usually turns out in the simplest situations to describe the physics via a Dirac delta function. In the end it boils down to the fact that the attractive inverse square potential doesn't exist in isolation, and one is led inevitably to add a Dirac delta function, whose coupling runs in the sense of renormalization group flow. Many otherwise not so clear features of the system become transparent once we have a Dirac delta function included, as we will see, for example : in this case the non-hermitian physics of pair creation comes in clearly through the imaginary coupling of the Dirac delta function.

3.1 Effective action and boundary condition

The effective action for the PPEFT for fall to the center in an attractive inverse square potential is, $S = S_B + S_b$, where S_B is the action for the Schrödinger bulk field, given by :

$$S_B = \int dt\ dQ \left[-\left(\frac{1}{2m} |\nabla|\psi|^2 + V(Q)|\psi|^2 \right) \right] \tag{3.1}$$

with $V(Q) = -\frac{\tilde{E}^2 + 1/4}{Q^2}$ and the action for the microscopic physics of the source at $Q = 0$ is given by :

$$S_b = \int dt\ dQ \mathcal{L}(\psi^*, \psi) \delta(Q) \tag{3.2}$$

At lowest order one can put, $\mathcal{L}_b(\psi^*, \psi) = -\lambda\psi^*\psi$. The field equations can be obtained by extremizing the action $\delta S = 0$, to obtain the Schrödinger equation

$$\left(\frac{d^2}{dQ^2} - U(Q)\right)\psi = -k^2\psi \tag{3.3}$$

with $U(Q) = -\frac{(\tilde{E}^2+1/4)}{Q^2} + \lambda\delta(Q)$, $-k^2 = -2m\mathcal{E}$. The boundedness of the wavefunction at $Q = 0$ can't be the right boundary condition to use because, as we will see in the next section, for small Q, both linearly independent wavefunction diverge as $Q \to 0$ similar to the wavefunction for $H(Q, P) = \frac{Q.P+P.Q}{2}$ [see Figure : 2 (b)], so we cannot necessarily choose one unambiguously. The weaker criteria of normalizability also turns out to be insufficient as demonstrated by Burgess et. al in [30]. Hence, one is led to derive the boundary condition from the properties of the source action, S_b.

The boundary condition as derived in [30] is obtained by integrating the above Schrödinger equation at the boundary in the limit $-\epsilon \leq Q \leq \epsilon$ giving :

$$\lambda = \left[\frac{\partial \ln(\psi)}{\partial Q}\right]_{Q=-\epsilon}^{Q=\epsilon} \tag{3.4}$$

The boundary condition is evaluated at $Q = \pm\epsilon$ because the description of PPEFT action breaks down at smaller distances compared to the actual radius of the source, $r = \epsilon$. The dependence of physical quantities on ϵ can be absorbed into an appropriate renormalization of the couping λ, which will be discussed in upcoming sections. This is where the story of renormalization comes in.

3.2 Scattering in 1D

Th Schrödinger equation for an attractive inverse square potential :

$$\left(-\frac{d^2}{dQ^2} - \frac{(1/4 + \tilde{E}^2)}{Q^2}\right)\chi(Q) = \mathcal{E}\chi(Q) \tag{3.5}$$

can be transformed to an Hankel type differential equation as illustrated in [30], with $\chi(Q) = \sqrt{z}u(z)$ and $z = kQ$:

$$z^2u'' + zu' + (z^2 - \sigma^2)u = 0 \tag{3.6}$$

where $\sigma^2 = -\tilde{E}^2$. The Hankel function of second kind, $H_\sigma^{(2)}(kQ)$ asymptotes at large Q to a left moving wave and the Hankel function of first kind $H_\sigma^{(1)}(kQ)$ asymptotes for large Q to a right moving wave (see Appendix B for properties of Hankel functions). The wavefunction of the above attractive inverse square potential is then given by :

$$\chi_+(Q) = \sqrt{kQ}\left(H_\sigma^{(2)}(kQ) + RH_\sigma^{(1)}(kQ)\right) \text{ for } Q \geq \epsilon \tag{3.7}$$

$$\chi_-(Q) = T\sqrt{kQ}H_\sigma^{(2)}(kQ) \text{ for } Q \leq -\epsilon \tag{3.8}$$

where, R and T are the reflection and transmission coefficients to be determined by boundary condition at $Q = \pm\epsilon$. The energy eigenfunction of the scale invariant squared Berry-Keating operator, $\phi(Q)$ will be small Q limit of $\chi(Q)$ (note that : $\phi(Q) = Q^{-1}\chi(Q)$) :

$$\phi_{\text{In+Ref}}(Q) = \frac{\left(\frac{-\left(\frac{kQ}{2}\right)^{i\tilde{E}}}{\Gamma(1+i\tilde{E})} + \frac{\exp(\pi\tilde{E})\left(\frac{kQ}{2}\right)^{-i\tilde{E}}}{\Gamma(1-i\tilde{E})}\right) + R\left(\frac{\left(\frac{kQ}{2}\right)^{i\tilde{E}}}{\Gamma(1+i\tilde{E})} - \frac{\exp(-\pi\tilde{E})\left(\frac{kQ}{2}\right)^{-i\tilde{E}}}{\Gamma(1-i\tilde{E})}\right)}{\sinh(\pi\tilde{E})\sqrt{kQ}}, \; Q \geq \epsilon \tag{3.9}$$

$$\phi_{Trans}(Q) = \frac{T}{\sinh(\pi\tilde{E})\sqrt{kQ}}\left(\frac{-1}{\Gamma(1+i\tilde{E})}\left(\frac{kQ}{2}\right)^{i\tilde{E}} + \frac{\exp(\pi\tilde{E})}{\Gamma(1-i\tilde{E})}\left(\frac{kQ}{2}\right)^{-i\tilde{E}}\right) \text{ for } Q \leq -\epsilon \tag{3.10}$$

Note that $\sigma = \pm i\tilde{E}$, is imaginary in this case unlike discussed for the 1D case in [30]. We have chosen $\sigma = -i\tilde{E}$ for the analysis.

To get one relation between R and T, we demand $\chi_+(\epsilon) = \chi_-(-\epsilon)$, to get

$$R - iT\exp(\pi\tilde{E}) = -\frac{H^{(2)}_{-i\tilde{E}}(k\epsilon)}{H^{(1)}_{-i\tilde{E}}(k\epsilon)} \tag{3.11}$$

For small $k\epsilon << 1$, the above relation can be written down as :

$$R - iT\exp(\pi\tilde{E}) = \frac{1 - X\exp(\pi\tilde{E})}{1 - X\exp(-\pi\tilde{E})} \tag{3.12}$$

where

$$X = \frac{\Gamma(1-\sigma)}{\Gamma(1+\sigma)}\left(\frac{k\epsilon}{2}\right)^{2\sigma} \tag{3.13}$$

We now calculate the coupling of the Dirac delta function using logarithmic derivative of the wavefunction at $Q = \pm\epsilon$ as given in Eq. (3.4) :

$$\lambda = \frac{\partial \ln(\phi_+(\epsilon))}{\partial x} - \frac{\partial \ln(\phi_-(-\epsilon))}{\partial x} \tag{3.14}$$

where $\phi_+(\epsilon)$ and $\phi_-(\epsilon)$ are the wavefunction in Eq. (3.9) and Eq. (3.10) evaluated at $Q = \pm\epsilon$:

$$\lambda = \frac{1}{\epsilon}\left(1 + i\tilde{E}\left[\frac{1 + X\exp(\pi\tilde{E}) - R(1 + X\exp(-\pi\tilde{E}))}{1 - X\exp(\pi\tilde{E}) - R(1 - X\exp(-\pi\tilde{E}))} + \frac{1 + X\exp(-\pi\tilde{E})}{1 - X\exp(-\pi\tilde{E})}\right]\right) \tag{3.15}$$

The coupling diverges as $\epsilon \to 0$, and therefore has to be renormalized. We must choose λ also to diverge in such a way that the observables, i.e reflection and transmission coefficients are ϵ- independent.
Redefining λ by :

$$\hat{\lambda} = 2\lambda\epsilon - 1 \tag{3.16}$$

and expanding Eq. (3.15) in powers of X in small $k\epsilon$ regime we obtain :

$$\hat{\lambda} = 2\mathrm{i}\tilde{E}\left[1 + X\exp(\pi\tilde{E})\left(\frac{1 - R\exp(-2\pi\tilde{E})}{1 - R}\right) + X\exp(-\pi\tilde{E}) + \mathcal{O}(X^2)\right] \tag{3.17}$$

Before, proceeding to calculate the reflection and transmission coefficients, we now pause to see how conservation loss depends on the nature of the Dirac delta function coupling.

3.2.0.1 Probability current

The probability flux is given by the expression :

$$J = \frac{i\hbar}{2m}\left(\phi\partial_x\phi^* - \phi^*\partial_x\phi\right) \tag{3.18}$$

where $\psi(x)$ is the energy eigenfunction. We use the boundary condition Eq. (3.4) to calculate the probability flux :

$$J(\epsilon) - J(-\epsilon) = \frac{i\hbar}{2m}(\lambda^* - \lambda)\phi^*(\epsilon)\phi(\epsilon) \tag{3.19}$$

It is clear from the above expression that, probability is conserved at the source if λ is real, i.e when $\lambda^* = \lambda$ or when probability of finding the particle is zero at the source. Otherwise, we have conservation loss at the source as is expected when pair creation occurs. As we will later see, it will be a source at the origin if $\Im(\lambda) > 0$ or a sink if $\Im(\lambda) < 0$.

3.2.0.2 Renormalization

In order to determine how the coupling λ must depend on ϵ to renormalize any divergences, we write down the renormalization evolution equation for the coupling of the Dirac delta potential, which can be calculated by taking the derivative with respect to ϵ keeping other physical quantities fixed, as given in [30] :

$$\epsilon\frac{d}{d\epsilon}\left(\frac{\hat{\lambda}}{2\sigma}\right) = \sigma\left(1 - \left(\frac{\hat{\lambda}}{2\sigma}\right)^2\right) \tag{3.20}$$

The renormalization group flow describes how the effective coupling within the point particle action must change for different values of ϵ in order to keep the physical quantities unchanged. The concept of renormalization is associated with studying the beta function whose zeros corresponds to the fixed points of the theory.

In this case the fixed points for the above equation for which the coupling $\hat{\lambda}$ does not evolve is given by : $\hat{\lambda} = \pm 2\sigma = \pm 2i\tilde{E}$. The renormalization group running of the parameter λ can have interesting consequences. The coupling of the Dirac delta function $\lambda = 0$ corresponds to $\hat{\lambda} = -1$, which is not a fixed point unless $\tilde{E} = -\frac{i}{2}$, but this value of $\tilde{E}$, corresponds to zero coupling of the attractive inverse square potential (note : the strength of the inverse square potential is $\tilde{E}^2 + 1/4$). Thus the Dirac delta function is *inevitable* for a non-zero attractive inverse square potential. Here, in this case of Schwinger pair creation problem, this *inevitable* Dirac delta function accounts for the non-hermitian physics that arises from pair creation. RG evolution for σ being imaginary is dealt with in detail in [27]. Integrating the above RG evolution equation using the initial condition $\lambda(\epsilon_0) = \lambda_0$, we get :

$$\frac{\hat{\lambda}}{2\sigma} = \frac{\frac{\lambda_0}{2\sigma} + \tanh(\sigma\ln(\epsilon/\epsilon_0))}{1 + \frac{\lambda_0}{2\sigma}\tanh(\sigma\ln(\epsilon/\epsilon_0))} \tag{3.21}$$

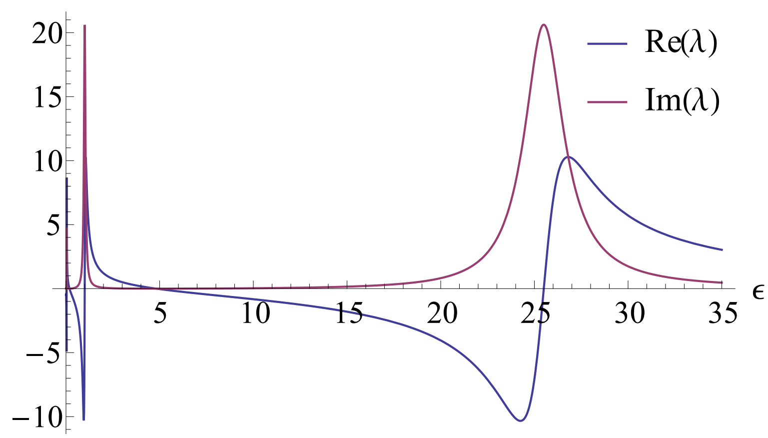

Figure 3.2: The plot for the real and imaginary parts of the renormalization group flow Eq. (3.21) for $\sigma = -i\tilde{E}$.

The Figure 3.2 portray this RG flow of the coupling $\hat{\lambda}$ as a function of ϵ. The flow picks a scale ϵ_* when $\Re(\hat{\lambda}) = 0$. Hence, it breaks the continuous scale invariance of the inverse square potential. The RG flow has different topology depending upon whether σ is real or imaginary as discussed in [27]. The Figure 3.3 shows the solution in the complex $\hat{\lambda}$ plane when σ is imaginary. The fixed points are isolated on the imaginary axis of the complex plane. As demonstrated in [27] these fixed points correspond to the scenarios of perfect absorber when $\Im(\lambda) < 0$ and a perfect emitter when $\Im(\lambda) > 0$. The connection of the fixed points to perfect absorption/emission comes from the fact that these amounts to choosing the coefficients C_+ or C_- of the wavefunction : $C_+ Q^{-1/2} \exp(i\tilde{E}\ln[Q]) + C_- Q^{-1/2} \exp(-i\tilde{E}\ln[Q])$ to vanish [27]. The choice of $C_+ = 0$ would correspond to only an in-falling wave and $C_- = 0$ would correspond to an out-going wave. The fact that the boundary conditions are related to the fixed points of the RG evolution, means that the process of emission/absorption is invariant under varying the position $Q = \epsilon$.

To calculate the reflection coefficient, we now use small ϵ expansion of the above equation [Eq. (3.21)] :

$$\frac{\hat{\lambda}}{2\sigma} = -1 - 2\left(\frac{\epsilon}{\epsilon_*}\right)^{2\sigma}, \ (\epsilon << \epsilon_*) \tag{3.22}$$

Reflection coefficient can then be computed by substituting the above expression of $\hat{\lambda}$ in Eq. (3.17) to obtain :

$$R = \frac{X_* \cosh(\pi\tilde{E}) - 1}{X_* \exp(-\pi\tilde{E}) - 1} \tag{3.23}$$

where ,

$$X_* = \frac{\Gamma(1-\sigma)}{\Gamma(1+\sigma)}\left(\frac{k\epsilon_*}{2}\right)^{2\sigma} \tag{3.24}$$

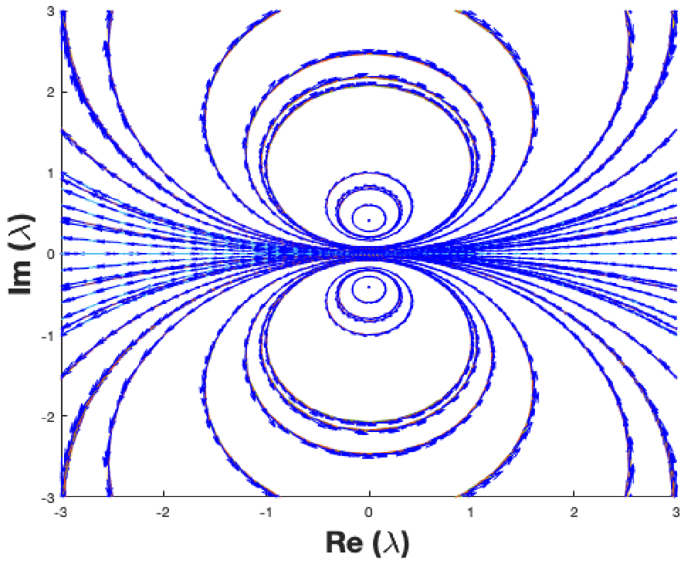

Figure 3.3: Phase portrait of the RG evolution given in Eq. (3.20) depicting the RG flow of $\hat{\lambda}$, which is related to the coupling of the Dirac delta function at the source. Arrows indicate the direction of the flow.

and using small $k\epsilon$ limit in Eq. (3.12) to get :

$$T = i\exp(-\pi\tilde{E})(1-R) = \frac{-iX_* \exp(-\pi\tilde{E})\sinh(\pi\tilde{E})}{X_* \exp(-\pi\tilde{E}) - 1} \tag{3.25}$$

It is clear from Eq. (3.25) that the unitarity condition is violated by an amount $\exp(-\tilde{E}\pi)$, unless $\tilde{E} = 0$. This is a signature of the Klein paradox. The paradox is reconciled by arguing that charged pairs are created at the origin. Probability conservation has to be recasted in terms of charge conservation.

CHAPTER 4

Eigenstates of quantum inverted harmonic oscillator

4.1 Energy eigenstates of the quantum inverted harmonic oscillator using a quantum canonical transformation

The incident and reflected wavefunction of IHO in the right hand side of the barrier in the ξ space can be obtained from the incident and reflected wavefunction of the inverse square potential in the Q representation [Eq. (3.9)] using the quantum generating function $\langle\xi|Q\rangle = \exp[\mathrm{i}F(Q,\xi)]$ [15,35], where $F(Q,\xi) = \frac{-\xi^2}{2} + \sqrt{2}\xi Q - \frac{Q^2}{2}$ is the classical generating function corresponding to the canonical transformation [Eq. (2.4)] (for details about quantum canonical transformation, see Appendix C) :

$$\langle\xi|\phi\rangle_{\text{Inc+Refl}} = \int dQ\ \langle\xi|Q\rangle\langle Q|\phi\rangle_{\text{Inc+Refl}} \tag{4.1}$$

$$= \int dQ\ \langle Q|\phi\rangle_{\text{Inc+Refl}} \exp\left(\mathrm{i}\left[\frac{-\xi^2}{2} + \sqrt{2}\xi Q - \frac{Q^2}{2}\right]\right) \tag{4.2}$$

$$= \frac{e^{-\frac{\tilde{E}\pi}{4}}}{\sinh(\pi\tilde{E})}\left[W(\tilde{E}, e^{-\mathrm{i}\pi/4}\sqrt{2}\xi) + R\,W(\tilde{E}, e^{i\pi/4}\sqrt{2}\xi)\right]$$

The integral in the Eq. (4.2) with the wavefunction of the inverse square potential in the Q-representation given in Eq. (3.9), can be identified with the integral representation of the parabolic cylinder function [36]. The eigenfunction $W(\tilde{E},\xi)$ is satisfied by the Schrödinger equation with an IHO potential [36]. The wavefunction in the ξ space is smooth in contrary to the wavefunction in the Q-representation [see Figure 4.1 and Figure 2.2 (b)]. Similarly one can obtain the transmitted wavefunction in the left hand side of the IHO barrier in the ξ space using the transmitted wavefunction of the inverse square potential in the Q-representation

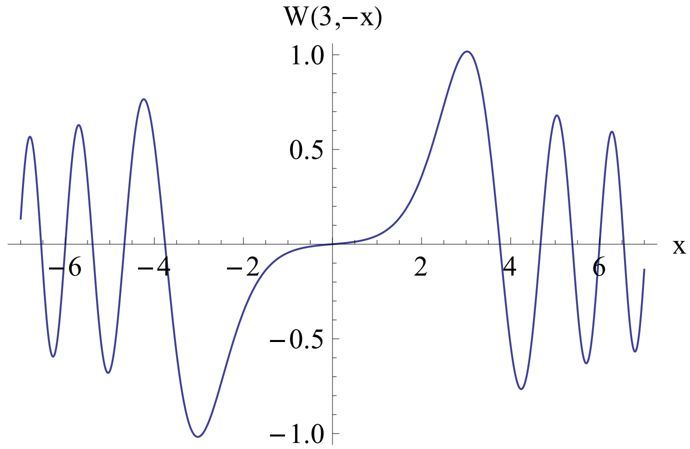

Figure 4.1: The energy eigenfunction of inverted harmonic oscillator in the ξ space : parabolic cylinder function $W(\tilde{E}, -x)$ with $\tilde{E} = 3$.

given in Eq. (3.10) :

$$\begin{aligned}
\langle\xi|\phi\rangle_{\text{Trans}} &= \int dQ\ \langle\xi|Q\rangle\langle Q|\phi\rangle_{\text{Trans}} \\
&= \int dQ\ \langle Q|\phi\rangle_{\text{Trans}} \exp\left(\mathrm{i}\left[\frac{-\xi^2}{2} + \sqrt{2}\xi Q - \frac{Q^2}{2}\right]\right) \qquad (4.3) \\
&= \frac{T\exp(-\pi\tilde{E})e^{-\frac{\tilde{E}\pi}{4}}}{\sinh(\pi\tilde{E})} W^*(\tilde{E}, e^{i3\pi/4}\sqrt{2}\xi) \qquad (4.4)
\end{aligned}$$

Note that the transmitted wavefunction is complex conjugated with respect to the refelected. The ratio of the reflection and the transmission coefficients for the IHO barrier follows :

$$\left|\frac{R}{T}\right| = e^{\tilde{E}\pi} \qquad (4.5)$$

which is the amplitude of produced pairs during tunneling through the barrier. In the next chapter we describe the Klein paradox.

Chapter 5

Klein paradox and pair production

Klein paradox is associated with the over reflection of charged particles from the barrier formed from an inhomogeneous electric field. We started off the problem with a relativistic dispersion relation and then mapped it onto an effective non-relativistic IHO problem. Klein paradox for Schwinger pair creation is demonstrated by constructing the asymptotic scattering branches of inverted harmonic oscillator with incident wave coming from the right side of the barrier and reflected wave going back to $+\infty$ and transmitted wave going to $-\infty$

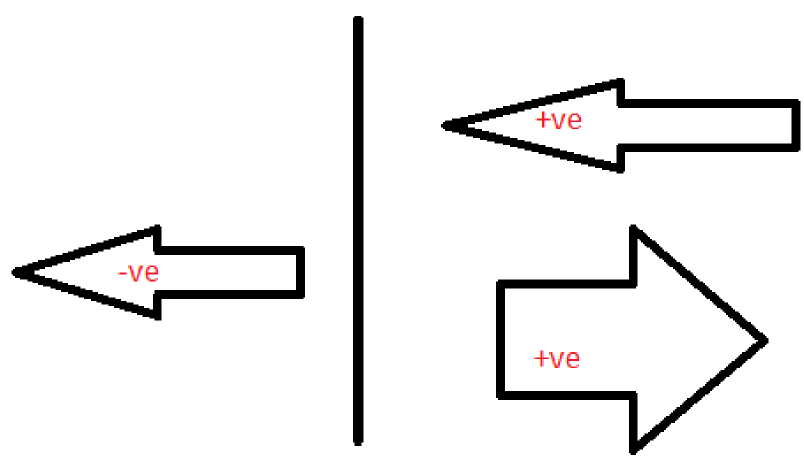

Figure 5.1: Klein paradox - over reflection of charged particles from a barrier formed from an inhomogeneous electric field. The figure shows incident and over reflected positively charged particles and transmitted anti-particles with negative charge.

given by :

$$\frac{1}{\sqrt{\sqrt{\frac{qE}{\hbar c}}\left(x+\frac{\hbar\omega}{qE}\right)}}\exp\left(\mathrm{i}\left(\frac{qE}{\hbar c}\right)^2\left(x+\frac{\hbar\omega}{qE}\right)^2-\mathrm{i}\tilde{E}\ln\left(\sqrt{\frac{qE}{\hbar c}}\left(x+\frac{\hbar\omega}{qE}\right)\right)\right)(x\to+\infty) \tag{5.1}$$

$$\frac{R}{\sqrt{\sqrt{\frac{qE}{\hbar c}}\left(x+\frac{\hbar\omega}{qE}\right)}}\exp\left(-\mathrm{i}\left(\frac{qE}{\hbar c}\right)^2\left(x+\frac{\hbar\omega}{qE}\right)^2+\mathrm{i}\tilde{E}\ln\left(\sqrt{\frac{qE}{\hbar c}}\left(x+\frac{\hbar\omega}{qE}\right)\right)\right)(x\to+\infty) \tag{5.2}$$

$$\frac{Te^{-\tilde{E}\pi}}{\sqrt{\sqrt{\frac{qE}{\hbar c}}\left(x+\frac{\hbar\omega}{qE}\right)}}\exp\left(\mathrm{i}\left(\frac{qE}{\hbar c}\right)^2\left(x+\frac{\hbar\omega}{qE}\right)^2-\mathrm{i}\tilde{E}\ln\left(\sqrt{\frac{qE}{\hbar c}}\left(x+\frac{\hbar\omega}{qE}\right)\right)\right)(x\to-\infty) \tag{5.3}$$

as described in [32]. In the chapter 3, we saw that the unitarity condition is violated [see Eq. (3.25)] due to the imaginary coupling of the Dirac delta function. Incident particles from the right side of the IHO barrier are overreflected from the barrier and particles are transmitted to the left side of the barrier. This is a clear signature of the Klein paradox [9]. In this thesis, instead of describing the physics at asymptotically large x, we also describe pair creation using the small Q physics of an attractive inverse square potential. The charge density then gives the proper charge assignments :

$$J_0 = (\omega + Ex)\phi^*\phi \tag{5.4}$$

For large negative x, we have anti-particles and for large positive x, we have particles. The statement of probability conservation $|R|^2 + |T|^2 = 1$, has to be interpreted as charge conservation :

$$\frac{1}{|R|^2} - \frac{|T|^2}{|R|^2} = 1 \tag{5.5}$$

The above equation can be viewed as $|\alpha|^2 - |\beta|^2 = 1$, with $|\alpha|^2 = \frac{1}{|R|^2}$ and $|\beta|^2 = \frac{|T|^2}{|R|^2}$.The RHS of Eq. [5.5] represents incident unit positive charge (particle) coming from the right side of the IHO barrier and $|\beta|^2 = \frac{|T|^2}{|R|^2}$ represents transmitted negative charge (anti-particle) to $+\infty$ and $|\alpha|^2-1$ is the increased flux of reflected wave necessary for charge conservation. The true resolution of Klein paradox would require a quantum field theory treatment because the effective single particle formalism is used to describe a multi particle phenomenon. Second quantized study of pair creation will be pursued as a separate work in the near future. Hence, constant electric field pair production is described as tunneling through the IHO barrier or as particles being produced at the origin of the inverse square potential.

Chapter 6

Parabolic cylinder functions as squeezed states

6.1 Generalized coherent states

There are three guiding characteristics for identifying a coherent state of the harmonic oscillator :

1. Coherent state ($|\alpha\rangle$) is an eigenstate of the harmonic oscillator annihilation operator
2. It is generated by the harmonic oscillator unitary group transformation on the vacuum state.
3. It is a minimum uncertainty state.

There are coherent states in other quantum systems, but they do not in general obey all the above three characteristics possessed by harmonic oscillator coherent states. In particular these methods, though equivalent for constructing harmonic oscillator coherent states, are not so, for other quantum systems. The defining property of a coherent state is a debatable issue.
Generalization based on (i) consists in defining a coherent state as an eigenstate of the annihilation operator of the underlying algebra. Coherent states so constructed are called Barut-Girardello coherent states in the literature. This approach is, however, restrictive as not all algebras contain an operator whose eigenvalue problem is solved by continuously labeled states.

Perelomov's definition of a coherent state [37] is clearly a generalization of property (ii). It holds for any algebra but ignores property (iii). In a given system, say if the operators $\hat{X}, \hat{Y}, \hat{Z}$ form a closed Lie algebra, then the Perelomov coherent states can be straightforwardly constructed. From the state $|y\rangle$ which is an eigenstate of Y : $Y|y\rangle = y|y\rangle$, the coherent state $|c,d\rangle$ can be constructed as :

$$|c,d\rangle = \exp(cX + dZ)|y\rangle \tag{6.1}$$

One can also construct coherent states from the eigenstates of other operators which will lead to different coherent states. As an example : consider the case of the $so(3)$ Lie algebra generated by orbital angular momentum operators, L_1, L_2 and L_3 given by the commutation relation $[L_i, L_j] = i\hbar\epsilon_{ijk}L_k$ where $i,j,k = 1,2,3$. Perelomov coherent state constructed from the eigenstate of L_3 : $L_3|m\rangle = m|m\rangle$,

$$|\phi_1, \phi_2\rangle = \exp(i(\phi_1 L_1 + \phi_2 L_2))|m\rangle \tag{6.2}$$

The initial state from which one constructs the coherent state by applying the unitary operator is called the *fiducial state* in the literature, which needs to be an eigenstate of an operator which forms the Lie algebra. For example, in the harmonic oscillator case, the vacuum state $|0\rangle$ is the fiducial state and in the above example of the $so(3)$ algebra, the state $|m\rangle$ is the fiducial state. In short, Perelomov's construction of coherent states gives a group theoretic generalization of the harmonic oscillator coherent states. Note that mathematically it amounts to constructing a group element from the underlying Lie algebra by exponentiation. For mathematical details and a justification about constructing Lie group elements from Lie algebra, see : [37, 38].There have been attempts to come up with a bridge between two of these methods of constructing coherent states [39].

6.2 Squeezed states and su(1,1) algebra

The su(1,1), non compact Lie algebra is of great interest in quantum optics. The su(1,1) algebra generated by the operators K_x, K_y and K_z is given by :

$$[K_x, K_y] = -iK_z, [K_y, K_z] = iK_x, [K_z, K_x] = iK_y \tag{6.3}$$

These commutation relation can be expressed in terms of $K_\pm = K_x \pm \mathrm{i}K_y$ and K_z as

$$[K_+, K_-] = -2K_z, [K_z, K_\pm] = \pm K_\pm \tag{6.4}$$

Now consider,

$$K_+ = \frac{(a^\dagger)^2}{2}, \quad K_- = \frac{a^2}{2}, \quad K_z = \frac{1}{2}(a^\dagger a + \frac{1}{2}) \tag{6.5}$$

where a and $a^\dagger$ are the usual creation and annihilation operators of the harmonic oscillator, satisfying $[a, a^\dagger] = I$. It can be clearly shown that they form a closed su(1,1) algebra

[Eq. (6.4)], using the commutation relations of the harmonic oscillator algebra $[\hat{a}, \hat{a}^\dagger] = \hat{I}$. The unitary operator in the Perelomov sense discussed in the previous section, given by Eq. (6.1), can be constructed to act on the eigenstate of $K_z = \frac{1}{2}\left(a^\dagger a + \frac{1}{2}\right)$ as,

$$|\eta\rangle = \exp(\eta(a^\dagger)^2 - \eta^* a^2)|0\rangle \tag{6.6}$$

It is interesting to note that this unitary operator in the Perelomov sense is the squeezing operator $S(\eta)$ and the state $|\eta\rangle$ is called the squeezed state [40]. The displacement operator which generates the coherent state from the vacuum state was constructed from harmonic oscillator algebra and the squeezing operator is *not* a part of the Heisenberg-Weyl group, but is constructed from the su(1,1) algebra formed by the operators given in Eq. (6.5) [40]. Interestingly, the following generators also form a closed $su(1,1)$ Lie algebra :

$$K_1 = \frac{1}{2}(p^2 - x^2),\ K_2 = \frac{1}{2}(p^2 + x^2),\ K_3 = \frac{1}{2}(x.p + p.x) \tag{6.7}$$

where K_1 is the IHO Hamiltonian, K_2 is the simple harmonic oscillator (SHO) Hamiltonian and K_3 is the Berry-Keating operator. The eigenvalue problem of the IHO Hamiltonian which generates the parabolic cylinder functions are well known to be $su(1,1)$ squeezed states as discussed in [31]. Equivalently, the integral representation of the wavefunction of IHO,

$$\begin{aligned}
\langle\xi|\phi\rangle_{\text{Trans}} &= \int dQ\ \langle\xi|Q\rangle\langle Q|\phi\rangle_{\text{Trans}} \\
&= \int dQ\ \langle Q|\phi\rangle_{\text{Trans}} \exp\left(\mathrm{i}\left[\frac{-\xi^2}{2} + \sqrt{2}\xi Q - \frac{Q^2}{2}\right]\right) \qquad (6.8) \\
&= \frac{T\exp(-\pi\tilde{E})e^{-\frac{\tilde{E}\pi}{4}}}{\sinh(\pi\tilde{E})} W^*(\tilde{E}, e^{i3\pi/4}\sqrt{2}\xi) \qquad (6.9)
\end{aligned}$$

can be seen as the Perelomov construction of SU(1,1) squeezed state. The quantum generating function $\exp[\mathrm{i}F(\xi,Q)] = \exp\left[\mathrm{i}\left(\frac{-\xi^2}{2} + \sqrt{2}\xi Q - \frac{Q^2}{2}\right)\right]$, can be seen as a group element generated by the generators of the above $su(1,1)$ Lie algebra. Hence pair creation under a static electric field can be viewed as being due to squeezing of the vacuum.

Chapter 7

Conclusion

In conclusion, we have demonstrated that the classical field theory of Schwinger pair creation with a static electric field can be described using an effective Schrödinger equation with an attractive inverse square potential constructed using the squared Berry-Keating operator, in the canonically rotated coordinates of the inverted harmonic oscillator. The large ξ physics of the inverted harmonic oscillator is equivalently described by small Q physics of the attractive inverse square potential. It appears that the inverse square potential by itself is not a fully specified eigenvalue problem. We use PPEFT to systematically derive the boundary condition using the source action which leads to an inevitable addition of Dirac delta function at the origin $Q = 0$, with imaginary coupling. The non-hermitian physics leads to conservation loss. Probability conservation is then reinterpreted as charge conservation. The su(1,1) Lie algebra generated by IHO Hamiltonian, SHO Hamiltonian and Berry-Keating operator gives us a hint that pair creation can be seen as arising due to squeezing of the vacuum.

CHAPTER 8

Future works

8.1 Pair creation and quantum caustics

8.1.1 Introduction to catastrophe theory

For this introductory section on singularities, caustics and its description using catastrophe theory, we follow the thesis by Wyatt Kirkby [41] and the book by Poston and Stewart [42]. A point $u = (u_1, u_2, .., u_n)$ is said to be a critical point of a function $f(x_1, x_2, .., x_n)\epsilon\mathbb{R}$ if

$$\left.\frac{\partial f}{\partial x_1}\right|_u = \left.\frac{\partial f}{\partial x_2}\right|_u = ... = 0 \tag{8.1}$$

It is a degenerate critical point if the Hessian is a singular matrix :

$$\det\left(\frac{\partial^2 f}{\partial x_1 \partial x_2}\right) = 0 \tag{8.2}$$

If Hessian matrix is non singular then the critical point u is called non-degenerate critical point. A critical point for which there exist no critical point within any deleted neighborhood of this point is called isolated critical point [41]. Control parameters are those tunable parameters that determine the global behavior of the function $f(x)$.

Theorem (Morse Lemma) :

For some isolated non-degenerate critical point $u\epsilon\mathbb{R}$ of the function $f : \mathbb{R}^n \to \mathbb{R}$, there exists a smooth transformation to some coordinate $y = (y_1, y_2, ..., y_n)$ in a neighborhood of u and for $y_i(u) = 0$ such that $f = f(u) - y_1^2 - y_2^2 - ... - y_l^2 + y_{l+1}^2 + ... + y_n^2$

Rank	Co-dimension (K)	Catastrophe function (Φ_K)
1	1	$s^3 + a_1 s$
1	2	$s^4 + a_2 s^2 + a_1 s$
1	3	$s^5 + a_3 s^3 + a_2 s^2 + a_1 s$
2	3	$s_1^2 s_2 + s_2^3 + a_3 s_1^2 + a_2 s_2 + a_1 s_1$

Table 8.1: The classification of catastrophe functions

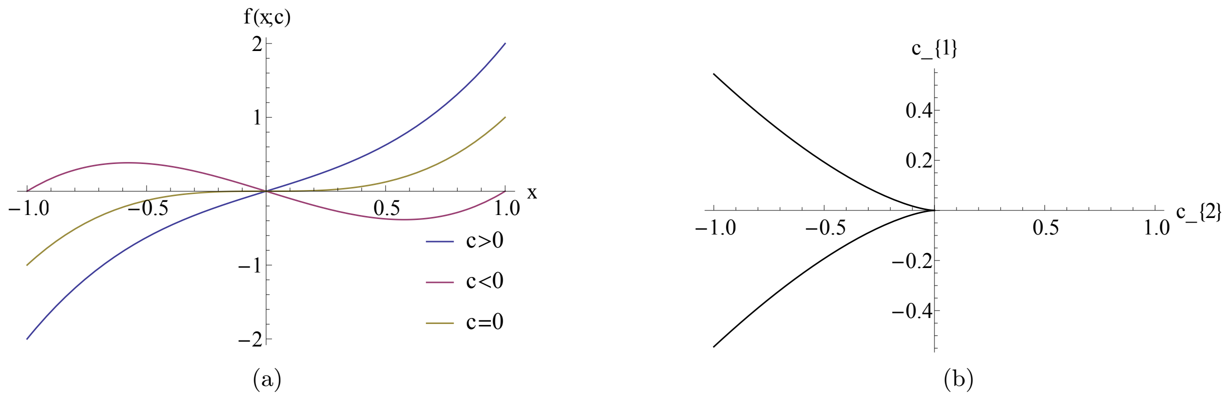

Figure 8.1: (a). Geometry of Fold catastrophe. The figure in (a) shows the disappearance (coalescence) of the critical points as we change c from negative to positive (b). Control space of cusp catastrophe

In the neighborhood of a degenerate critical point u, the function

$$f(y;c) = \sum_{i=1}^{k} \lambda_i(c) y_i^2 + f_{NM}(y_{k+1}, ..., y_n; c) \tag{8.3}$$

In the neighborhood of $(u;c)$ with f_{NM} taking the form of the so-called catastrophe functions or catastrophe [41]. Classification of such catastrophes are given by Arnold based on the number of state variables and its rank.

Theorem(Thom's theorem) :

Local to a neighborhood of an isolated critical point of the function f, can be locally described by catastrophe function with the appropriate number of state variables and rank.

Eg : (1). The Fold catastrophe with single control parameter c is defined as

$$f(x;c) = x^3 + cx \tag{8.4}$$

Critical points lie in $x^2 = -c/3$. There exists a bifurcation at $c = 0$, where the number of critical points change from 2 to 0 [see Figure 8.1 (a)].

2.) The Cusp catastrophe with two control parameters c_1, c_2 is defined by :

$$C(x; c_1, c_2) = x^4 + c_2 x^2 + c_1 x \tag{8.5}$$

The critical points are determined by : $4x^3 + 2c_2 x + c_1 = 0$. Solving $\frac{dC}{dx} = 0$ and $\frac{d^2C}{dx^2} = 0$, we get the cusp curve [see Figure : 8.1 (b)] :

$$c_1 = \pm\sqrt{\frac{8}{27}}(-c_2)^{3/2} \tag{8.6}$$

In the context of studying the nature and properties and dynamics of light, geometric ray theory describe light propagation in terms of rays. When light rays focus at a particular point, the regions of focusing are called ray caustics. Examples of ray caustics include many natural phenomenon like : rainbow, whirls under swimming pool [43], cusp structure inside a coffee mug etc.

Optics of Rainbow : It is an excellent example of ray caustic. Caustics, which are envelope of family of rays, are singularities of the geometric ray theory. As described in [43], the intensity of light in the geometric ray theory is given by :

$$I \propto \left| \frac{x}{\sin(D)} \left(\frac{dD}{dx}\right)^{-1} \right| \tag{8.7}$$

where D is the angle of deviation of a ray incident on the rain drop with impact parameter x. Deviation of indent ray on the drop is given by :

$$D = \pi - 4r + 2i = \pi - 4\arcsin(x/n) + 2\arcsin(x) \tag{8.8}$$

The above intensity diverges at the rainbow angle $D(x_{\min})$, i.e where $\frac{dD}{dx} = 0$. But, in reality we don't see infinite intensity in the nature. Hence, some feature not in the domain of ray theory should be responsible for smoothening of this singularity. Interference and diffraction of light are not in the domain of ray theory and hence incomplete. We must resort to wave theory of light to describe these effects.

8.1.2 Wave/Diffraction catastrophes

Diffraction integral is given by :

$$\Psi_K(a) = \int ds e^{i\Phi(s,a)} \tag{8.9}$$

Ψ_K results in the smoothing of the singularities associated with the ray catastrophes, Φ_K. Eg: Fold catastrophe (Φ_1) is associated with Airy function (Ψ_1) [see Table 8.2].
Another class of catastrophes, called logged caustics, recently proposed has the form :

$$I(k, a, a_0) = \int_C dt \exp\left(ikf(t, a, a_0)\right)) \tag{8.10}$$

Catastrophe function, $\Phi(s,a)$	Diffraction catastrophe, Ψ_K	Diffraction integral
$s^3 + a_1 s$	$\int ds \exp(i[s^3 + a_1 s])$	Airy function
$s^4 + a_2 s^2 + a_1 s$	$\int ds \exp(i[s^4 + a_2 s^2 + a_1 s])$	Pearcey function
$s^2 + a_0 \ln(s)$	$\int ds \exp(i[s^2 + a_0 \ln(s)])$	Logged gaussian integral
$s^3 + a_1 s + a_0 \ln(s)$	$\int ds \exp(i[s^3 + a_1 s + a_0 \ln(s)])$	Logged Airy integral

Table 8.2: Examples of some diffraction catastrophes and its integral representation

where $f(t,a,a_0) = t^{K+2} + \sum_{m=L}^{K} a_m t^m + a_0 \ln(t)$ are called logged caustics.

One can identify these wave catastrophes or diffraction integrals as wavefunctions in quantum mechanics. Airy and Pearcey function are known to appear in quantum many body physics [41]. Interestingly these diffraction integrals takes the form analogous to Feynman's path integral

$$\Psi(x,t) = \int \mathcal{D}x \exp(iS/\hbar)\psi_0(x) \tag{8.11}$$

The diffraction integral corresponding to the fold caustic is an Airy function. By scaling the catastrophe function by

$$y^3 = -\frac{s^3}{3}, z = -3^{1/3} a_1 \tag{8.12}$$

one can write the wavefunction upto a smooth change of variables at a fold caustic as :

$$\Psi(z) = \frac{1}{2\pi}\int_{-\infty}^{\infty} ds \exp\left(i\left[zs - \frac{s^3}{3}\right]\right) = \mathrm{Ai}[z] \tag{8.13}$$

where $Ai[z]$ is the Airy function of first kind. It is well known that Airy function satisfies the following second order differential equation :

$$\frac{d^2\psi}{dz^2} - z\psi = 0 \tag{8.14}$$

The caustic divides the wavefunction to two regions, with $z < 0$ where amplitude oscillates and $z > 0$ where it decays exponentially [see Figure 8.2].

We saw that geometric ray theory of a rainbow exhibits singularities. In the wave theory the intensity of light for the rainbow is given by an Airy function :

$$\mathrm{Ai}(x) = \int_0^{\infty} ds \cos\left(\frac{s^3}{3} + xs\right) \tag{8.15}$$

where, x is the rainbow crossing variable. The ray caustic is smoothened by wave effects. Airy further realized that this diffraction integral describes the wave close to any caustic, not just a rainbow. Corresponding to a fold caustic, the diffraction integral is an Airy function.

8.1.3 Quantum catastrophe

In the previous section we saw that the singularities of ray theory are smoothened by wave effects. Quantum caustics are singularities of the underlying wave theory, characterized

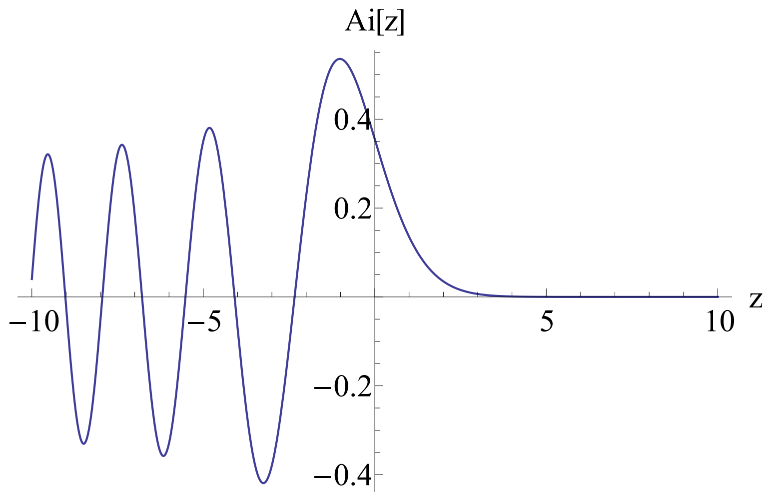

Figure 8.2: Plot of Airy function showing oscillatory behavior for $z < 0$ and exponential decay for $z > 0$.

by logarithmic phase singularities of the form $F(Q) \approx Q^{i\nu} \exp(-i\omega t)$ with $\Re(\nu) \neq 0$ [34]. Quantum catastrophes may be responsible for quantum effects, for example, pair creation from the quantum vacuum. Interestingly we saw that such singularities do appear in the Schwinger pair creation problem in the canonically rotates (Q, P) coordinates [see chapter 2. Eq. (2.7)]. Such logarithmic phase singularities are well known to appear in the waves near an event horizon of a black hole, accelerated frames etc. It is still not known whether these quantum caustics admits a classification similar to classical catastrophes.
The goal of this project would be to see if non-hermitian bifurcation occurs in the case of Schwinger pair creation and to see if the quantum caustics admit a classification scheme similar to diffraction catastrophes.

8.2 Superlenses and fall to the center

According to the Rayleigh criterion, the resolution of a standard lens is limited by the wavelength of light. However, over the years there have been a number of ingenious proposals for beating this limit. For example, the 2014 Nobel prize in Chemistry was awarded to Betzig, Hell and Moerner, for the development of vortex beams of light for super-resolved fluorescence microscopy which greatly improves the imaging of molecules inside living cells. Another approach is provided by "superlenses". These include Maxwell's fish eye lens (MFEL), the Luneburg lens and the Eaton lens [44]. MFEL is spherically symmetric and has a refractive index n that varies as a function of radius r as $n(r) \propto 1/(1 + r^2)$. It is not like a standard lens because it does not magnify and both the source and image must be contained within the lens but it has infinite resolution. This is possible because it has the special property that, in the words of Maxwell [45] "all the rays proceeding from any point in the medium will meet accurately in another point". To illustrate this property a water wave analogue was recently proposed, called Maxwell's fish eye pond [46], where the ripples from a stone thrown anywhere into the pond are turned around to re-converge again and the process repeats. The technological applications of such a lens include integrated optics on a chip for aberration free imaging [47] and also perfect coupling of two atoms (qubits) that are imbedded in the lens but on opposite sides [48]. There are number of proposals for how to build MFEL using graded photonic crystals [49] and plasmon optics [48]. However, the theory behind MFEL is subtle and controversial, with some researchers doubting that it can really provide perfect focusing [50,51]. My goal in this project is to resolve this controversy by using point particle effective field theory (PPEFT) [30].

My interest in superlenses comes from a seemingly unrelated problem, namely "fall to the center" in quantum mechanics. This occurs when a quantum particle moves in an inverse square potential of the form $V(r) = -g/r^2$. When $g > J^2/2m$, where J is the angular momentum, the particle falls to the center of the potential. The main subject of this thesis was mapping an inverted harmonic oscillator Hamiltonian to a Hamiltonian with an inverse square potential [chapter 2]. As we saw, this problem is notorious because, unlike the closely related Coulomb potential where $V(r) = -g/r$ which can be put into the Schrödinger equation and solved exactly (to describe the energy levels and stable orbitals of the electron in a hydrogen atom), the $1/r^2$ problem is poorly defined and leads to non-hermitian behavior where the particle is absorbed/produced at the origin. Hermiticity is usually considered a fundamental requirement of probability conservation and indicates that the inverse square potential problem is incomplete as stated and must be supplemented by extra boundary conditions. However, in recent work [27], it was shown that PPEFT can treat loss/gain systems where particles are lost or produced (such as occurs, e.g. near black holes). Now, optics and quantum mechanics are closely related theories because they both describe waves obeying a wave equation. It turns out that the MFEL refractive index profile is equivalent to Schrödinger's equation with an inverse square potential and thus the two problems are fundamentally related.

The goal of this project will be to use PPEFT to analyze MFEL and related superlenses. There are some hints that superlenses may have loss and gain as a fundamental part of their operation: another way to realize superlenses is by using new artificial materials called metamaterials that work by amplifying exponentially small signals that get lost in propagation between source and lens [52]. The first phase of the project would be to develop a PPEFT that provides a simple and systematic approach to deal with the gain and loss associated with the MFEL and hence resolve the current controversy. Although theoretical in nature, this project may contribute to the realization of a useful optical device. The second phase of the project would be to test the theoretical results, using numerical ray tracing simulation techniques. The ray tracing method is a powerful way of analyzing optical behavior in lenses with varying refractive index and also absorption.

Appendix A

Self-adjointness and von-Neumann deficiency indices

Self-adjointness is often not distinguished from hermiticity in the physics literature. The distinction is usually thought to be purely mathematical.

Definition (Self adjoint operator) : An operator A is said to be self-adjoint if it satisfies the following :

1. $A = A^{\dagger}$: this is the usual symmetric or Hermitian condition.

2. The domain, $D(A) = D(A^{\dagger})$

Theorem due to von-Neumann gives a recipe to check if an Hermitian operator is self-adjoint or not. The von-Neumann deficiency indices (n_{+}, n_{-}) counts the number of square integrable solution to the eigenvalue problem given by [12] :

$$H\psi_{\pm} = \pm i\lambda\psi_{\pm} \tag{A.1}$$

Theorem (von- Neumann's test) :

- Operator H is essentially self adjoint iff $n_{+} = n_{-} = 0$

- Operator H has self adjoint extensions iff $n_{+} = n_{-} \neq 0$

- Operator H is not self adjoint if $n_{+} \neq n_{+}$

We consider two examples to illustrate the calculation of the deficiency indices, i.e. particle in a box and particle in half real line with standard momentum operator and Berry-Keating operator.

A.1 Particle in a box

Let us consider the example of the particle in a box to illustrate the concept of self-adjoint extension. Potential of the partice in a box is given by :

$$V(x) = \begin{cases} 0, & \text{if } -L < x < L \\ \infty, & \text{otherwise} \end{cases}$$

The Schrödinger equation is given by :

$$-\frac{\hbar^2}{2m}\frac{d^2\psi}{dx^2} = E\psi, \quad -L < x < L \tag{A.2}$$

Let's check if the momentum operator is self-adjoint in the finite interval :

$$\left(\psi, -i\hbar\frac{d}{dx}\phi\right) - \left(-i\hbar\frac{d\psi}{dx}, \phi\right) = -i\hbar\left(\psi^*(L)\phi(L) - \psi^*(-L)\phi(-L)\right) \tag{A.3}$$

It implies that the momentum is a Hermitian (symmetric) operator, but not necessarily self-adjoint. The adjoint, $P_\theta = -i\hbar\frac{d}{dx}$ acts on the subspace of $\mathcal{L}^2[-L, L]$, with functions following :

$$\phi(L) = \exp(i\theta)\phi(-L) \tag{A.4}$$

As discussed above, deficiency indices are $(n_+, n_-) = (1, 1)$ and hence von-Neumann's test says the momentum operator admits self-adjoint extensions. The $\theta = 0$ corresponds to the usual periodic boundary condition imposed for the particle in a box mentioned in textbooks. The case of anti-periodic boundary condition corresponding to $\theta = \pi$ is dealt in detail with signatures of spontaneous symmetry breaking proposed in [14]. Apart from these two cases, in general momentum operator for particle in a box admits infinite self-adjoint extensions.

A.2 Particle in half real line

In this section we review the deficiency indices for the standard momentum operator and the Berry-Keating operator in half real line ($\mathbb{R}^+$) and full real line ($\mathbb{R}$). The deficiency indices for the momentum operator are calculated by counting the number of normalizable solutions to

$$p\psi_\pm = \pm i\lambda\psi_\pm \tag{A.5}$$

, for real $\lambda > 0$. For the momentum operator, $p = -i\frac{d}{dx}$, the solutions are

$$\psi_\pm \approx \exp(\pm\lambda x) \tag{A.6}$$

Hence, for $x \in \mathbb{R}^+$, the deficiency indices for the momentum operator, $(n_+, n_-) = (0, 1)$. It is in contrast to the momentum operator in a finite interval which admits self adjoint extensions. Hence, the standard momentum operator is not physical in $\mathbb{R}^+$.
For the Berry-Keating operator

$$p_{BK} = \frac{x.p + p.x}{2} \tag{A.7}$$

the solutions of the eigenvalue problem Eq. (A.1) are

$$\psi_\pm \approx x^{\mp\lambda - \frac{1}{2}} \tag{A.8}$$

The Berry-Keating operator is then essentially self-adjoint in $\mathbb{R}^+$ with the deficiency indices $(n_+, n_-) = (0, 0)$. The Berry-Keating operator however is not self-adjoint in the full real line ($\mathbb{R}$) with deficiency indices $(n_+, n_-) = (1, 0)$. Since the Berry-Keating operator is physical on half line, we introduce Heaviside step function when writing the wavefunction in chapter 2 of the thesis [see Eq. (2.9 and Eq. (2.7)].
Hence, we can use the Euler operator which generates scale transformations (we have $[x, p_{BK}] = i\hbar x$) :

$$\exp(i\alpha p_{BK}/\hbar)x \exp(-i\alpha p_{BK}/\hbar) = x \exp(\alpha) \tag{A.9}$$

as an effective momentum operator in the half real line [33]:

$$\exp(i\alpha p_{BK}/\hbar)x_{BK} \exp(-i\alpha p_{BK}/\hbar) = x_{BK} + \alpha \tag{A.10}$$

The Berry-Keating operator $p_{BK} = \frac{x.p+p.x}{2}$ with new position operator $x_{BK} = \ln(x)$, satisfies Heisenberg algebra $[x_{BK}, p_{BK}] = \mathrm{i}$. The new momentum operator p_{BK} with its canonically conjugate position variable x_{BK} generates a hyperbolic phase space.

The list of some of the relevant operators and their deficiency indices discussed above :

- Hamiltonain of the free particle in full real line, $\mathbb{R}$ is essentially self adjoint with deficiency indices $(n_+, n_-) = (0, 0)$

- Momentum of particle in the interval $[-a, a]$ has deficiency indices $(n_+, n_-) = (2, 2)$. Hence it admits self adjoint extensions.

- The standard momentum operator $-i\frac{d}{dx}$ is non self adjoint in the half real line $\mathbb{R}^+$ with deficiency indices $(n_+, n_-) = (0, 1)$

- The Berry-Keating operator discussed in this thesis, $\frac{x.p+p.x}{2}$ is essentially self adjoint in the half line with deficiency indices $(n_+, n_-) = (0, 0)$.

Hence, a symmetric differential operator acting on a given space of functions need not be a self-adjoint operator, it might admit none or infinity of self-adjoint extensions. As demonstrated in the above example of particle in a box, self-adjoint extension can be arbitrary.

Appendix B

Properties of Hankel function

In this appendix we state some of the properties of the Hankel function that is used in the main body of the thesis.

Hankel function are satisfied by the Bessel differential equation given by :

$$z^2u'' + zu' + (z^2 - \sigma^2)u = 0 \tag{B.1}$$

The Hankel function of first kind and second kind are definedd by :

$$H_\sigma^{(1)}(z) = J_\sigma(z) + iN_\sigma(z) \tag{B.2}$$

and

$$H_\sigma^{(2)}(z) = J_\sigma(z) - iN_\sigma(z) \tag{B.3}$$

where J_σ is the Bessel function and N_σ is the Neumann function. The Hankel function of first kind, $H_\sigma^{(1)}(z)$ asymptotes at large z to :

$$H_\sigma^{(1)}(z) \approxeq \sqrt{\frac{2}{\pi z}} \exp\left[\mathrm{i}\left(z - \frac{\pi\sigma}{2} - \frac{\pi}{4}\right)\right] \tag{B.4}$$

The Hankel function of second kind $H_\sigma^{(2)}(z)$ asymptotes for large z to :

$$H_\sigma^{(2)}(z) \approxeq \sqrt{\frac{2}{\pi z}} \exp\left[-\mathrm{i}\left(z - \frac{\pi\sigma}{2} - \frac{\pi}{4}\right)\right] \tag{B.5}$$

The reflection properties of Hankel functions that are used in chapter 3 are :

$$H_\sigma^{(1)}(\exp(i\pi)z) = -\exp(-i\pi\sigma)H_\sigma^{(2)}(z) \tag{B.6}$$

and similarly,

$$H_\sigma^{(2)}(\exp(-i\pi)z) = -\exp(i\pi\sigma)H_\sigma^{(1)}(z) \tag{B.7}$$

For small z Hankel functions reduces to :

$$H_\sigma^{(1)}(z) \approxeq \frac{1}{i\sin(\pi)\sigma}\left(\frac{1}{\Gamma(1-\sigma)}\left(\frac{z}{2}\right)^{-\sigma} - \frac{\exp(-i\pi\sigma)}{\Gamma(1+\sigma)}\left(\frac{z}{2}\right)^{\sigma}\right) \tag{B.8}$$

$$H_\sigma^{(2)}(z) \approxeq \frac{1}{i\sin(\pi)\sigma}\left(-\frac{1}{\Gamma(1-\sigma)}\left(\frac{z}{2}\right)^{-\sigma} + \frac{\exp(i\pi\sigma)}{\Gamma(1+\sigma)}\left(\frac{z}{2}\right)^{\sigma}\right) \tag{B.9}$$

Appendix C

Theory of quantum canonical transformation

In classical mechanics, canonical transformations are those change of variables which preserve the Poisson bracket structure : $\{p,x\} = 1, \{p,p\} = \{q,q\} = 0$. The quantum canonical transformation are those change of variables which preserves the quantum condition: $[x,p] = i\hbar, [x,x] = [p,p] = 0$. The quantum generating function analog of the classical generating function is defined as [15] :

$$\exp(iF_1(\xi,Q,t)) \equiv \langle\xi|Q\rangle \tag{C.1}$$

Similarly one can define other types of generating functions $\exp(iF_2(\xi,P,t)) = \langle\xi|P\rangle$, and so on [35]. The generating functions in classical mechanics are related by Legendre transformation whereas the quantum generating functions are related by Fourier transform. For example :

$$\exp(iF_2(\xi,P)) = \langle\xi|P\rangle = \int dQ\langle\xi|Q\rangle\langle Q|P\rangle = \int dQ \exp(iF_1(\xi,Q))\exp(iQP) \tag{C.2}$$

Wavefunction in ξ representation of a state $|\phi\rangle$ can be obtained from the wavefunction in Q representation using the quantum generating function as :

$$\langle\xi|\phi\rangle = \int dQ\langle\xi|Q\rangle\langle Q|\phi\rangle = \int dQ \exp(iF_1(\xi,Q))\langle Q|\phi\rangle \tag{C.3}$$

Interestingly, $\exp(iF_1(\xi,Q))$ satisfies a quantum Hamilton-Jacobi equation whose c-number form for the Hamiltonian $H = \frac{p^2}{2m} + V(\xi)$ can be written as [35]:

$$\frac{1}{2}\left(\frac{\partial F_1}{\partial \xi}\right)^2 - \frac{i\hbar}{2}\frac{\partial^2 F_1}{\partial \xi^2} + V(\xi) = -\frac{\partial F_1}{\partial t} \tag{C.4}$$

where, the second term is called the quantum potential. Clearly, in the limit $\hbar \to 0$, the above quantum Hamilton-Jacobi equation is reduced to the classical Hamilton-Jacobi equation. It has been a known fact that writing the wavefunciton as $\langle \xi | \phi \rangle = \exp(iS(\xi, t))$, we can get the Hamilton-Jacobi equation where $S(\xi, t)$ is interpreted as a complex valued phase of the wavefunction which generates trajectories, but here, in the theory of quantum canonical transformation it acquires much more significance. The function $F_1(\xi, Q, t)$ which is used to calculate the wavefunction using Eq. (C.3), is the quantum counterpart of the classical generating function [35].

Appendix

D

Sauter potential and broken scale invariance

In this section we attempt to regularize the inverted harmonic oscillator which fall off to infinity by introducing a length scale after which the electric field is turned off, i.e by using a Sauter potential [53]. The Klein-Gordon equation [Eq. (2.1)], modified with the Sauter potential, $A_t = EL\tanh\left(\frac{x}{L}\right)$ gets mapped onto an effective time independent Schrödinger equation with Rosen-Morse barrier (See Figure D.1:) :

$$\left(\frac{-\hbar^2}{2m}\frac{\partial^2}{\partial x^2} - \frac{1}{2}m\left(\frac{qEL}{mc}\right)^2\left(\tanh\left(\frac{x}{L}\right) + \frac{\hbar\omega}{qEL}\right)^2\right)\langle x|\psi\rangle = \frac{-mc^2}{2}\langle x|\psi\rangle \tag{D.1}$$

Under the coordinate transformation $y = L\tanh\left(\frac{x}{L}\right)$, the above Schrödinger equation transforms as :

$$\left(\frac{-\hbar^2}{2m}\left(\left(1-\left(\frac{y}{L}\right)^2\right)\frac{d}{dy}\right)^2 - \frac{m}{2}\left(\frac{qE}{mc}\right)^2\left(y + \frac{\hbar\omega}{qE}\right)^2\right)\langle y|\Psi\rangle = \frac{-mc^2}{2}\langle y|\Psi\rangle \tag{D.2}$$

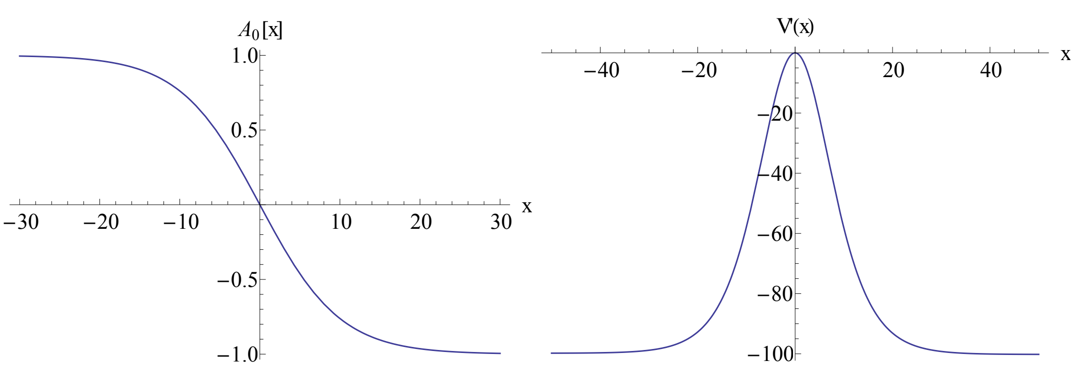

Figure D.1: Sauter potential and Rosen-Morse barrier with length scale $L = 10$.

It is clear that the above Schrödinger equation has broken scale invariance. When $L \to \infty$, the Sauter potential reduces to the standard Schwinger case (see Figure 1). The Rosen-Morse barrier in the effective Schrödinger picture reduces to an IHO potential in the limit $L \to \infty$. The above Schrödinger equation is written in terms of the new momentum operator $\Pi_y = (1-y^2)p_y$ which is self adjoint in the domain $y \in (-1,1)$ by von-Neumann's theorem, follows : $[(1-y^2)p_y, \tanh^{-1}(y)] = -i$. The above differential equation [Eq. (D.2)] can be written as an effective Schrödinger (or Helmholtz equation) equation in the y coordinate using the integrating factor with :

$$V_{eff}^{RM} - \tilde{\epsilon} = -\frac{1/L^2}{1-(\frac{y}{L})^2} - \frac{y^2(1/L^4 + \frac{m}{2}(\frac{qE}{mc})^2) - \epsilon}{(1-(\frac{y}{L})^2)^2} \tag{D.3}$$

For $L \to \infty$, the effective potential reduces to IHO potential as expected. Doing an analytic continuation $L \to \mathrm{i}L$, and in the limit of large L and asymptotically large y, the Schrödinger equation becomes :

$$\left(\frac{-d^2}{dy^2} + \frac{1}{L}\delta(y) - \frac{\left(1 + L^4 \frac{m}{2}\left(\frac{qE}{mc}\right)^2\right)}{y^2} \right) \Psi(y) = 0 \tag{D.4}$$

Upon undoing the analytical continuation, the Schrödinger equation for the Schwinger case becomes :

$$\left(\frac{-d^2}{dy^2} + \frac{\mathrm{i}}{L}\delta(y) - \frac{\left(1 + L^4 \frac{m}{2}\left(\frac{qE}{mc}\right)^2\right)}{y^2} \right) \Psi(y) = 0 \tag{D.5}$$

The above Helmholtz equation can be written as a Schrödinger equation with attractive inverse square potential and Dirac delta barrier with imaginary coefficient as :

$$\left(\frac{-d^2}{dy^2} + \frac{\mathrm{i}}{L}\delta(y) - \frac{\left(1 + L^4 \frac{m}{2}\left(\frac{qE}{mc}\right)^2\right)}{y^2} \right) \Psi(y) = \tilde{\mathcal{E}}\Psi(y), \tag{D.6}$$

with $\tilde{\mathcal{E}} \to 0$. The above Schrödinger equation is also *non-hermitian* describing conservation loss. Interestingly, this regularization of the Schwinger problem also gives rise to a Dirac delta function with a imaginary coupling which has $1/L$ dependence. This choice of regularization is one among many available choices.

Bibliography

[1] Robert Brout, Serge Massar, Renaud Parentani, and Ph Spindel. A primer for black hole quantum physics. *Physics Reports*, 260(6):329–446, 1995.

[2] K Srinivasan and T Padmanabhan. Particle production and complex path analysis. *Physical Review D*, 60(2):024007, 1999.

[3] NL Balazs and A Voros. Wigner's function and tunneling. *Annals of Physics*, 199(1):123–140, 1990.

[4] W Heisenberg. Remarks on the dirac theory of the positron. *Z. Phys.*, 90:692–692, 1934.

[5] W Heisenberg and H Euler. Consequences of dirac theory of the positron. *arXiv preprint physics/0605038*, 2006.

[6] Richard P Feynman. The theory of positrons. *Physical Review*, 76(6):749, 1949.

[7] Julian Schwinger. On gauge invariance and vacuum polarization. *Physical Review*, 82(5):664, 1951.

[8] Gerald V Dunne. The heisenberg-euler effective action: 75 years on. In *International Journal of Modern Physics: Conference Series*, volume 14, pages 42–56. World Scientific, 2012.

[9] A Calogeracos and Norman Dombey. History and physics of the klein paradox. *Contemporary physics*, 40(5):313–321, 1999.

[10] V Kasper, Florian Hebenstreit, MK Oberthaler, and J Berges. Schwinger pair production with ultracold atoms. *Physics Letters B*, 760:742–746, 2016.

[11] G Barton. Quantum mechanics of the inverted oscillator potential. *Annals of Physics*, 166(2):322–363, 1986.

[12] Michael Reed and Barry Simon. *II: Fourier Analysis, Self-Adjointness*, volume 2. Elsevier, 1975.

[13] Vanilse S Araujo, Francisco Antônio Bezerra Coutinho, and J Fernando Perez. Operator domains and self-adjoint operators. *American Journal of Physics*, 72(2):203–213, 2004.

[14] Anton Z Capri. Self-adjointness and spontaneously broken symmetry. *American Journal of Physics*, 45(9):823–825, 1977.

[15] Paul Adrien Maurice Dirac. On the analogy between classical and quantum mechanics. *Reviews of Modern Physics*, 17(2-3):195, 1945.

[16] N Mukunda. Dynamical symmetries and classical mechanics. *Physical Review*, 155(5):1383, 1967.

[17] Robert A Leacock and Michael J Padgett. Hamilton-jacobi/action-angle quantum mechanics. *Physical Review D*, 28(10):2491, 1983.

[18] Robert A Leacock and Michael J Padgett. Quantum action-angle-variable analysis of basic systems. *American Journal of Physics*, 55(3):261–264, 1987.

[19] RS Bhalla, AK Kapoor, and PK Panigrahi. Energy eigenvalues for a class of one-dimensional potentials via quantum hamilton–jacobi formalism. *Modern Physics Letters A*, 12(05):295–306, 1997.

[20] Michael V Berry and Jonathan P Keating. H= xp and the riemann zeros. In *Supersymmetry and Trace Formulae*, pages 355–367. Springer, 1999.

[21] C Yuce, A Kilic, and A Coruh. Inverted oscillator. *Physica Scripta*, 74(1):114, 2006.

[22] EM Lifshitz, LD, and Sykes Landau (JB). *Quantum Mechanics; Non-relativistic Theory*. Pergamon Press, 1965.

[23] Aaron K Grant and Jonathan L Rosner. Classical orbits in power-law potentials. *American Journal of Physics*, 62(4):310–315, 1994.

[24] Christopher C Gerry. Coherent states and the kepler-coulomb problem. *Physical Review A*, 33(1):6, 1986.

[25] KM Case. Singular potentials. *Physical Review*, 80(5):797, 1950.

[26] Danny Birmingham, Kumar S Gupta, and Siddhartha Sen. Near-horizon conformal structure of black holes. *Physics Letters B*, 505(1-4):191–196, 2001.

[27] Ryan Plestid, CP Burgess, and DHJ O'Dell. Fall to the centre in atom traps and point-particle eft for absorptive systems. *Journal of High Energy Physics*, 2018(8):59, 2018.

[28] LP Pitaevskii and A Rosch. Breathing modes and hidden symmetry of trapped atoms in two dimensions. *Physical Review A*, 55(2):R853, 1997.

[29] Kumar S Gupta and SG Rajeev. Renormalization in quantum mechanics. *Physical Review D*, 48(12):5940, 1993.

[30] CP Burgess, Peter Hayman, Matt Williams, and László Zalavári. Point-particle effective field theory i: classical renormalization and the inverse-square potential. *Journal of High Energy Physics*, 2017(4):106, 2017.

[31] G Satya Prakash and GS Agarwal. Mixed excitation-and deexcitation-operator coherent states for the su (1, 1) group. *Physical Review A*, 50(5):4258, 1994.

[32] R Parentani and R Brout. Vacuum instability and black hole evaporation. *Nuclear Physics B*, 388(2):474–508, 1992.

[33] J Twamley and GJ Milburn. The quantum mellin transform. *New Journal of Physics*, 8(12):328, 2006.

[34] Tamas Kiss and Ulf Leonhardt. Towards a classification of wave catastrophes. *Journal of Optics A: Pure and Applied Optics*, 6(5):S246, 2004.

[35] J-H Kim and H-W Lee. Canonical transformations and the hamilton-jacobi theory in quantum mechanics. *Canadian journal of physics*, 77(6):411–425, 1999.

[36] Frank WJ Olver, Daniel W Lozier, Ronald F Boisvert, and Charles W Clark. *NIST handbook of mathematical functions hardback and CD-ROM*. Cambridge university press, 2010.

[37] Askold Perelomov. *Generalized coherent states and their applications*. Springer Science & Business Media, 2012.

[38] Das Ashok and Okubo Susumu. *Lie groups and Lie algebras for physicists*. World Scientific, 2014.

[39] P Shanta, S Chaturvedi, V Srinivasan, GS Agarwal, and CL Mehta. Unified approach to multiphoton coherent states. *Physical review letters*, 72(10):1447, 1994.

[40] Ravinder R Puri. *Mathematical methods of quantum optics*, volume 79. Springer Science & Business Media, 2001.

[41] Wyatt Kirkby. Singularities in many-body quantum dynamics. Master's thesis, 2017.

[42] Tim Poston, Ian Stewart, and RH Plaut. Catastrophe theory and its applications. *Journal of Applied Mechanics*, 46(2):524–532, 1979.

[43] Michael Victor Berry. Nature,Äôs optics and our understanding of light. *Contemporary Physics*, 56(1):2–16, 2015.

[44] Ulf Leonhardt. Perfect imaging without negative refraction. *New Journal of Physics*, 11(9):093040, 2009.

[45] J C Maxwell. Some solutions of problems. *Camb. Dublin Math. J.*, 8:188, 1854.

[46] Paul Kinsler, Jiajun Tan, Timothy CY Thio, Claire Trant, and Navin Kandapper. Maxwell's fishpond. *European Journal of Physics*, 33(6):1737, 2012.

[47] O Bitton, R Bruch, and U Leonhardt. Two-dimensional maxwell fisheye for integrated optics. *Physical Review Applied*, 10(4):044059, 2018.

[48] Janos Perczel, Péter Kómar, and Mikhail D Lukin. Quantum optics in maxwell's fish eye lens with single atoms and photons. *Physical Review A*, 98(3):033803, 2018.

[49] Fabian Gaufillet and Eric Akmansoy. Maxwell fish-eye and half-maxwell fish-eye based on graded photonic crystals. *IEEE Photonics Journal*, 10(3):1–10, 2018.

[50] Tomáš Tyc and Xiang Zhang. Forum optics: Perfect lenses in focus. *Nature*, 480(7375):42, 2011.

[51] M. Alonso. Is the maxwell-shafer lens able to form super-resolved images? *New J. Phys.*, 17:073013, 2015.

[52] John Brian Pendry. Negative refraction makes a perfect lens. *Physical Review Letters*, 85(18):3966, 2000.

[53] Barry R Holstein. Strong field pair production. *American Journal of Physics*, 67(6):499–507, 1999.